- 1 A highly versatile fungal glucosyltransferase for specific production of
- 2 quercetin-7-O-β-D-glucoside and quercetin-3-O-β-D-glucoside in different
- 3 hosts
- 4
- 5 Jie Ren¹† Wenzhu Tang¹,2† Caleb Don Barton¹ Owen M Price³ Mark Wayne Mortensen¹
- 6 ◆ Alexandra Phillips¹ ◆ Banner Wald¹ ◆ Simon Elgin Hulme¹ ◆ Logan Powell Stanley¹ ◆ Joan
- 7 Hevel³ Jixun Zhan¹

8

- 9 ¹ Department of Biological Engineering, Utah State University, 4105 Old Main Hill, Logan,
- 10 UT 84322-4105, USA
- ² School of Biological Engineering, Dalian Polytechnic University, Dalian, Liaoning 116034,
- 12 China
- ³ Department of Chemistry and Biochemistry, Utah State University, 0300 Old Main Hill,
- 14 Logan, UT 84322-0300, USA

15

[†] These authors contributed equally to this work.

17

- 18 Correspondence: Jixun Zhan
- iixun.zhan@usu.edu

20

Abstract

22

23

24

25

26

27

28

29

30

31

32

33

34

35

36

37

38

39

40

41

Glycosylation is an effective way to improve the water solubility of natural products. In this work, a novel glycosyltransferase gene (BbGT) was discovered from Beauveria bassiana ATCC 7159 and heterologously expressed in *Escherichia coli*. The purified enzyme was functionally characterized through in vitro enzymatic reactions as a UDP-glucosyltransferase, converting quercetin to five monoglucosylated and one diglucosylated products. The optimal pH and temperature for BbGT are 35 °C and 8.0, respectively. The activity of BbGT was stimulated by Ca²⁺, Mg²⁺ and Mn²⁺, but inhibited by Zn²⁺. BbGT enzyme is flexible and can glycosylate a variety of substrates such as curcumin, resveratrol, and zearalenone. The enzyme was also expressed in other microbial hosts including Saccharomyces cerevisiae, Pseudomonas putida, and Pichia pastoris. Interestingly, the major glycosylation product of quercetin in E. coli, P. putida, and P. pastoris was quercetin-7-O-β-D-glucoside, while the enzyme dominantly produced quercetin-3-O-β-D-glucoside in S. cerevisiae. The BbGT-harboring E. coli and S. cerevisiae strains were used as whole-cell biocatalysts to specifically produce the two valuable quercetin glucosides, respectively. The titer of quercetin-7-O- β -D-glucosides was 0.34 ± 0.02 mM from 0.83 mM quercetin in 24 hours by BbGT-harboring E. coli. The yield of quercetin-3-O- β -D-glucoside was 0.22 \pm 0.02 mM from 0.41 mM quercetin in 12 hours by BbGTharboring S. cerevisiae. This work thus provides an efficient way to produce two valuable quercetin glucosides through the expression of a versatile glucosyltransferase in different hosts.

Key points

- A highly versatile glucosyltransferase was identified from *B. bassiana* ATCC 7159.
- BbGT converts quercetin to five mono- and one di-glucosylated derivatives in vitro.
- Different quercetin glucosides were produced by BbGT in *E. coli* and *S. cerevisiae*.
- 45 **Keywords** Quercetin-7-O-β-D-glucoside · quercetin-3-O-β-D-glucoside
- 46 glucosyltransferase · heterologous expression · Beauveria bassiana ATCC 7159

Introduction

Glycosylation is a common reaction that plays a vital role in the formation of natural glucosides with various applications (Vogt and Jones 2000). The reaction is catalyzed by dedicated glycosyltransferases (GTs). GTs transfer specific sugar moieties from activated donor molecules, mainly nucleoside diphosphate sugars (NDP-sugars), to various acceptor molecules, including many plant secondary metabolites (Yonekura - Sakakibara and Hanada 2011). Sugar moieties play an irreplaceable role in many life processes such as cell differentiation, development, immunity, aging, carcinogenesis, and information transmission (Jiang et al. 2008). Moreover, the bioavailability, water solubility and stability of natural products can be enhanced through glycosylation, which may further modulate their biological activities (Dou et al. 2019; Mfonku et al. 2020; Yang et al. 2018). For example, the intracellular anti-oxidative activity of apigenin was improved by C-glycosylation (Wen et al. 2017); the stability of quercetin-3-O-rutinoside (rutin) in aqueous solution at 100 °C is higher than its aglycon quercetin and its degradation rate in phosphate buffer with Fe²⁺ and Cu²⁺ is slower (Ikeda and Taguchi 2010; Makris and Rossiter 2000). Therefore, glycosylation is a commonly used tool for developing new therapeutic agents.

Many natural products such as quercetin, curcumin and resveratrol are commonly used as dietary supplements due to their health benefits. However, these plant polyphenols often have low water solubility and poor bioavailability. For example, quercetin is a representative antioxidant flavonoid that exists in green tea, fruits and leaf vegetables. It exerts promising pharmacological properties, such as anticancer, anti-inflammatory, antiviral, and antihypertensive properties (Cai et al. 2013; Ma et al. 2013). However, poor water solubility hinders its health benefits on humans (Li et al. 2004). Therefore, it is imperative for researchers to discover an effective approach to improve its aqueous solubility. Quercimeritrin (quercetin-7-O-β-D-glucoside) is a natural quercetin glucoside reportedly having *in vitro* anti-

inflammatory activity (Anuradha and Sukumar 2013). It possesses strong antioxidant activity, with an oxygen radical absorbance capacity (ORAC) value of 18 ± 4 μmol Trolox® equivalents (TE)/μmol (Legault et al. 2011). Another glucoside of quercetin, isoquercitrin (quercetin-3-O-β-D-glucoside), has significant pharmacological activities against cancer, oxidative stress, cardiovascular disorders, diabetes and allergic reactions (Chen et al. 2015; Valentová et al. 2014). Isoquercitrin showed higher inhibitory effect than quercetin in an *ex vivo* angiogenesis assay (Matsubara et al. 2004). Paulke et al. found that isoquercitrin has better bioavailability than quercetin (Paulke et al. 2012). Specifically, isoquercitrin gavage provides higher quercetin metabolite levels in both tissues (double to five-fold) and plasma (double to three-fold), compared to the quercetin gavage (Day et al. 2001).

While chemical synthesis of glycosides often requires extensive group protection and deprotection and use of toxic reagents, biological glycosylation through GTs represents a green and selective way to prepare desired glycosides (Cheng et al. 2019). Many researchers have worked on exploring various GTs from microorganisms or plants to increase the water solubility and bioavailability of bioactive compounds (Méndez and Salas 2001). Ko et al. found a GT named BcGT-1 from *Bacillus cereus* which can glycosylate different flavonoids such as quercetin, apigenin, and genistein (Hyung Ko et al. 2006). Zhao et al. isolated a flavonoid GT CsUGT73A20 from a tea plant *Camellia sinensis*, which exhibits a broad substrate tolerance toward multiple flavonoids (Zhao et al. 2017). Therefore, nature provides a variety of GTs that can be used to prepare glycosides of natural products. However, like other enzymes, GTs usually have high selectivity and strict substrate specificity that often only function on a particular substrate and its analogs, which limit their use as versatile biocatalysts in enzymatic preparation of desired glycosides. As such, discovery of flexible GTs would add new tools for the synthesis of various glycosides.

Beauveria bassiana ATCC 7159 is a filamentous fungus that has been extensively used for biotransformation of bioactive molecules (Grogan and Holland 2000). Different reactions can be catalyzed by this strain, such as oxidation, reduction, hydrolysis, methylation, hydroxylation, and glycosylation. We have previously used B. bassiana ATCC 7159 to prepare various glucosides from diverse molecules such as anthraquinones and curcuminoids (Zeng et al. 2010; Zhan and Gunatilaka 2006a; Zhan and Gunatilaka 2006b). The strain can selectively introduce a glucose or 4'-O-methylglucose moiety to a phenolic hydroxyl group in the substrates. In this work, we cloned the dedicated GT (BbGT) from B. bassiana ATCC 7159 and expressed it in four heterologous hosts. BbGT was functionally characterized through in vitro reactions. It is highly versatile and can convert quercetin into five monoglucosylated and one diglucosylated products (Fig. 1). Furthermore, it can accept a variety of substrates, thus representing a useful enzymatic tool for glycosylation. Interestingly, when expressed in different hosts, the enzyme generated different major glycosylation products of quercetin, which provides a convenient way to prepare different quercetin glucosides using BbGT.

Materials and methods

General equipment and experimental materials

Products were analyzed and purified on an Agilent 1200 HPLC instrument with an Agilent Eclipse Plus-C18 column (5 μ m, 250 mm × 4.6 mm). The samples were eluted with methanol-water (20:80 to 80:20, v/v, containing 0.1% formic acid) at a flow rate of 1 mL/min for 30 minutes. ESI-MS spectra were obtained on an Agilent 6130 single quadrupole LC-MS in the negative mode. 1D and 2D NMR spectra were recorded in deuterated dimethyl sulfoxide (DMSO- d_6) on a Bruker Avance III HD Ascend-500 NMR instrument (500 MHz for ¹H NMR and 125 MHz for ¹³C NMR) in the Department of Chemistry and Biochemistry, Utah State University. The chemical shift (δ) values are described in parts per million (ppm) and coupling

constants (J values) are reported in hertz (Hz). MicroPulserTM electroporation apparatus (Bio-Rad, USA) was used for electroporation.

Phusion® High-Fidelity DNA polymerase, restriction enzymes and T4 DNA ligase were purchased from New England Biolabs. Resibufogenin, tetracycline, quercetin, curcumin, resveratrol and zearalenone were purchased from Sigma-Aldrich (USA). Indigoidine was produced and purified in our lab (Xu et al. 2015; Yu et al. 2013). HisPur™ Ni-NTA resin and Luria-Bertani (LB) medium were purchased from Thermo Fisher Scientific (Rockford, IL, USA). Bradford assay solution was purchased from TCI America (Portland, OR, USA). Solvents and all other chemicals were purchased from Fisher Scientific. Milli-Q water was used throughout this study.

Strains, vectors, media, and culture condition

B. bassiana ATCC 7159, Saccharomyces cerevisiae BJ5464, Pseudomonas putida KT2440 and Pichia pastoris GS115 were obtained from the American Type Culture Collection (ATCC). E. coli XL1-Blue and BL21(DE3) were purchased from Agilent for gene cloning and protein expression, respectively. The pJET1.2 (Thermo Fisher Scientific, USA) together with pET28a(+) (Millipore Sigma, USA), pPICZB (Thermo Fisher Scientific, USA), YEpADH2p-URA3 (provided by Yi Tang at the University of California, Los Angeles) and pMiS1-mva-ges (provided by Jens Schrader and Josef Altenbuchner at Dechema-Forschungsinstitut and University of Stuttgart) vectors were, respectively, used for gene cloning and expression of the Bbgt gene. All primers were synthesized by Thermo Fisher Scientific. Carbenicillin (50 μg/mL), kanamycin (50 μg/mL), and zeocin (50 μg/mL) were supplemented into the culture media for selection of correct clones when appropriate. Wild type B. bassiana was grown in YM medium (BD Biosciences, USA) at 28 °C for 3 days in order to extract the genomic DNA. The E. coli strains were routinely grown in LB medium (Fisher Scientific, USA) at 37 °C. Synthetic complete (SC) (uracil dropout 0.77 g/L, yeast nitrogen base 6.7 g/L and glucose 20

g/L) and YP (1% yeast extract and 2% peptone) medium were used to grow *S. cerevisiae* BJ5464. *P. pastoris* was grown in YPDS medium (1% yeast extract, 2% peptone, 2% filtersterilized glucose and 1 M sorbitol). MGY medium (glycerol 10 g/L, yeast nitrogen base 6.7 g/L and biotin 0.4 mg/L) and MM medium (yeast nitrogen base 13.4 g/L and biotin 0.4 mg/L) were used for *P. pastoris* protein expression.

Phylogenetic analysis

For the phylogenetic analysis, the full-length amino acid sequence of BbGT was aligned with 19 GTs from other species such as plants, bacteria, and fungi using online version of Clustal Omega. The resulting alignment was used to construct an unrooted phylogenetic tree using the neighbor-joining method.

Cloning of the Bbgt gene from B. bassiana and plasmids construction

The genomic DNA was extracted from *B. bassiana* using the Quick-DNATM Fungal/Bacterial Microprep Kit (Zymo Research, USA) according to the manufacturer's instructions. To amplify the *Bbgt* gene (1,386 bp), the primers (1 μM), genomic DNA (0.2 μL), dNTP mix (200 μM), 5× bufer (4 μL), DMSO (0.4 μL), Phusion[®] High-Fidelity DNA Polymerase (0.2 μL at 2 U/μL) and nuclease-free water were mixed to bring the volume to 20 μL. The PCR was performed by an initial denaturation at 98 °C for 5 minutes, followed by 20 cycles of touchdown program (98 °C for 30 seconds, annealing at 65 °C for 40 seconds, decreasing 0.5 °C per cycle, and extension at 72 °C for 90 seconds), and then 20 cycles of regular program (98 °C for 30 seconds, annealing at 55 °C for 40 seconds, and extension at 72 °C for 90 seconds), and finally, 72 °C for 10 minutes of extension.

The PCR product was purified using a 0.8% agarose gel with a GeneJET Gel Extraction Kit (Thermo Fisher Scientific, USA) and ligated into the pJET1.2 cloning vector to yield pWZ7 (pJET1.2-*Bbgt*). The ligation product was transferred into *E. coli* XL1-Blue competent cells

through chemical transformation, and the transformants were selected on an LB agar plate with 50 µg/mL carbenicillin. After digestion check and sequencing, the gene was then excised from pWZ7 and ligated to the pET28a expression vector between the *Nde*I and *Eco*RI restriction enzyme sites to yield expression plasmid pWZ8 (pET28a-*Bbgt*), and the YEpADH2p-URA3 expression vector between *Nde*I and *Pml*I to yield pWZ9 (YEpADH2p-URA3-*Bbgt*).

The same gene was also PCR amplified from pWZ8 using different primers (Table 1) and ligated into pJET1.2 cloning vector, yielding pJR10 (pJET1.2-*Bbgt*). The *Bbgt* gene was excised from pJR10 and ligated into the pPICZB expression vector between the *Eco*RI and *Not*I restriction enzyme sites and pMIS1-*mva*-*ges* expression vector between the *Pme*I and *Hin*dIII sites to yield expression plasmids pJR14 (pPICZB -*Bbgt*) and pJR16 (pMiS1-*Bbgt*), respectively (Table 1). Sequences were confirmed by using the Sanger method.

Heterologous expression of BbGT and *in vivo* biotransformation of quercetin in *E. coli* BL21(DE3)

The expression plasmid pWZ8 was introduced into *E. coli* BL21(DE3) through chemical transformation. A colony of *E. coli* BL21(DE3)/pWZ8 was picked into 5 mL of LB medium containing kanamycin (50 μg/mL), which was incubated at 37 °C with shaking (250 rpm) for about 12 hours. Then 500 μL of the seed culture was inoculated into 50 mL of LB broth containing kanamycin (50 μg/mL) with shaking at 250 rpm and 37 °C until an OD₆₀₀ between 0.4 and 0.6 was reached. Protein expression was induced with 200 μM isopropyl β-D-1-thiogalactopyranoside (IPTG) (Gold Biotechnology, USA) at 28 °C for an additional 16 hours with shaking at 250 rpm. After protein expression, 0.4 mM quercetin and 0.11 M glucose were added for product analysis. The culture was maintained at 28 °C and 250 rpm for an additional 2 days. The culture was then extracted three times with 50 mL of ethyl acetate and subjected to analysis on the LC-MS at 350 nm.

Purification of BbGT from E. coil BL21(DE3)/pWZ8

E. coil BL21(DE3)/pWZ8 cells were harvested by centrifugation at 3,000 ×g and 4 °C for 10 minutes, and subsequently washed twice with distilled water and resuspended in lysis buffer including 20 mM Tris-HCl buffer (pH 7.9) and 0.5 M NaCl with 1 mM dithiothreitol. The harvested cells were disrupted by ultrasonication (Misonix Sonicator 3000, Misonix Inc., USA) on ice. The cell lysates were centrifuged at 10,000 ×g and 4 °C for 10 minutes to collect the soluble fraction containing target protein and analyzed by sodium dodecyl sulfate-polyacrylamide gel electrophoresis (SDS-PAGE) as soluble fraction. SDS-PAGE analysis used a premixed protein marker (EZ-RunTM Pre-Stained Rec Protein Ladder, molecular range: 11-170 kDa, Fisher BioReagents) as the reference. After electrophoresis, the gel was stained with 0.1% Coomassie Brilliant Blue R250, and destained in 20 % (v/v) acetic acid-water.

To purify the enzymes, the supernatant from the cell lysates was loaded onto a HisPurTM Ni-NTA affinity column (Thermo Scientific, Rockford, USA) according to the manufacturer's protocol. After eluting the column with cold (4 °C) washing buffers (50 mM Tris-HCl, 2 mM EDTA, 10 mM and 25 mM imidazole, pH 7.9), the recombinant BbGT was finally eluted with elution buffer (50 mM Tris-HCl, 2 mM EDTA, pH 7.9) containing 250 mM imidazole. The purified His6-tagged protein was concentrated and then desalted by buffer A (50 mM Tris-HCl, 2 mM EDTA, pH 7.9) using the 30 K Macrosep Advance Centrifugal Device (Pall Corporation, New York, USA). This enzyme was stored in 50% (v/v) glycerol at -20 °C. The protein concentration was determined using the Bradford assay. All purification steps were carried out at 4 °C.

Functional characterization of BbGT through in vitro enzymatic reactions

BbGT catalyzes the reaction of UDP-glucose with quercetin. Enzymatic assays were performed in a 100-μL reaction system, containing 20 mM Tris-HCl (pH 8.0), 2.5 mM substrate, 1 mM

MgCl₂, 2 mM sugar donor (uridine diphosphate glucose or UDP-glucose), and 12.5 μg of purified recombinant BbGT protein. The mixtures were thoroughly mixed and incubated at 30 °C for 6 hours, and then terminated by the addition of 200 μL of HPLC-grade methanol. The reaction mixtures were centrifuged at 13,000 $\times g$ for 10 minutes, and supernatants were collected to analyze the products by LC-MS as described before under 350 nm.

To investigate the substrate specificity of BbGT, several sugar-acceptor substrates were tested, including curcumin, resveratrol, tetracycline, zearalenone, resibufogenin, and indigoidine. Besides UDP-glucose, another structurally similar sugar-donor substrate, UDP-glucoric acid, was also reacted with quercetin. Reaction products were analyzed by LC-MS.

Homology modeling of BbGT

A homology model for BbGT was generated with the Swiss-Model server using the GT structure from a macrolide glycosyltransferase (PDB ID 2IYA) as a template. The homology model was aligned to UDP-glucose:flavonoid 3-O-glycosyltransferase (VvGT1), which glycosylates quercetin. Structures of VvGT1 with quercetin bound (PDB ID 2C9Z) and UDP-2-deoxy-2-fluoro glucose bound (PDB ID 2C1Z) were used to position the two molecules in the homology model.

Determination of the optimal in vitro reaction conditions

The standard curves were established using isolated quercetin glucosides to quantify product formation and conversion rate by HPLC. To determine the optimum reaction temperature, the reaction mixtures with quercetin as the substrate were incubated at varying temperatures (10, 20, 25, 30, 35, 40, 45, and 50 °C) for 3 hours. Glucosylation reactions were performed as described before. To find out the optimum pH for BbGT, this enzyme was reacted with quercetin at 35 °C in 200 mM phosphate buffer with different pH values (pH 4.5, 5.5, 6.0, 6.5, 7.0, 7.5, 8.0, and 8.5). For metal ions testing, CaCl₂, MgCl₂, MnCl₂, and ZnCl₂ were tested.

Control group did not contain any added metal ions. The assays were performed with individually divalent metal ion (10 mM, final concentration) using UDP-glucose as sugar donor and quercetin as sugar acceptor. All reactions were performed in triplicate and values were expressed as the mean \pm standard deviation.

Heterologous expression of BbGT and in vivo biotransformation of quercetin in S.

cerevisiae BJ5464

241

242

243

244

245

246

247

248

249

250

251

252

253

254

255

256

257

258

259

260

261

262

263

264

The expression plasmid pWZ9 was introduced into S. cerevisiae BJ5464 by LiAc transformation as described in the literature (Yu et al. 2017). The correct transformant was selected by autotrophy of uracil (Ura). Briefly, 10 µg of plasmid was mixed with 100 µL of S. cerevisiae BJ5464 competent cells in 700 µL of LiAc (100 mM Lithium Acetate, pH 7.5) / 40% PEG 3350 (120 mM PEG-3350) / TE (10 mM Tris-HCl, pH 7.5 and 1 mM EDTA) solution. The mixture was incubated at 28 °C for 30 minutes with shaking. 88 µL of DMSO was then added and mixed evenly, followed by 42 °C heat shock for 7 minutes. After centrifugation for 10 seconds at 13,000 ×g, the supernatant was discarded and cells were resuspended in 1 mL of TE buffer. The last step was repeated once and the cells were finally resuspended in 100 μL of TE buffer and spread on SC plates, which were incubated at 28 °C for 3 days. Yeast strains harboring plasmid pWZ9 was cultured in 5 mL of SC medium with shaking at 250 rpm and 28 °C overnight. Then 500 µL of seed culture was inoculated into 50 mL of SC medium in a 250mL Erlenmeyer flask, which was incubated at 28 °C and 250 rpm overnight. After the OD₆₀₀ value reached 1.0, 50 mL of YP medium was added and incubated overnight. Finally, 0.4 mM quercetin was added the next day and the cultures were maintained under the same conditions for an additional 2 days.

Heterologous expression of BbGT and in vivo biotransformation of quercetin in P. putida

KT2440

The expression plasmid pJR16 was introduced into *P. putida* KT2440 by electroporation as described in literature (Fidan and Zhan 2019). The cells were plated on LB agar plates containing 50 μg/mL kanamycin and incubated at 28 °C overnight. The transformants were picked and grown in 50 mL LB with 50 μg/mL kanamycin at 28 °C and 250 rpm. When the OD₆₀₀ reached 0.35, 100 mg L-rhamnose was added for induction at 28 °C and 250 rpm. After 16 hours, 0.4 mM quercetin and 0.11 M glucose were added into the culture for product analysis, which was incubated at 28 °C and 250 rpm for an additional 2 days.

Heterologous expression of BbGT and in vivo biotransformation of quercetin in P. pastoris

GS115

The expression plasmid pJR14 was linearized by PmeI and introduced into *P. pastoris* GS115 by electroporation as described in the literature (Cregg and Russell 1998; Lin-Cereghino et al. 2005). After electroporation, 1 mL of ice-cold 1 M sorbitol was added to the cuvette immediately. The mixture was then transferred to a sterile 15-mL tube and incubated at 30 °C without shaking for 2 hours. 200 μ L of the mixture was spread on YPDS agar plates containing various concentrations of ZeocinTM (10, 25, 50, 100, 200 μ g/mL). The plates were incubated at 30 °C for 3 days.

Colonies only appeared on the YPDS plate with 10 μg/mL ZeocinTM. A single colony of *P. pastoris* GS115/pJR14 was inoculated into MGY medium as seed culture and cultivated at 30 °C and 250 rpm for 24 hours. Then 1 mL of seed culture was inoculated into 50 mL of MGY medium, which was cultivated at 30 °C and 250 rpm for an additional 18 hours. The culture was centrifuged at 3,000 × g for 5 minutes, washed with MM medium twice and suspended in MM medium to be OD₆₀₀ 1.0. Afterwards, 50 mL of broth was transferred into a 500-mL shake flask and cultivated at 30 °C and 250 rpm. Methanol was fed every 24 hours to keep its concentration around 1%. After protein expression, 0.4 mM quercetin and 0.11 M

289 glucose were added, and the culture was maintained at 28 °C and 250 rpm for an additional 3 days.

Extraction, analysis, and purification of compounds

The cultures of *E. coli* BL21(DE3)/pWZ8 and *S. cerevisiae* BJ5464/pWZ9 were scaled up to 400 mL as described above, respectively. The biotransformation broths were maintained at 28 °C and 250 rpm for two days. Both cultures were extracted with 400 mL of ethyl acetate three times. The extracts were dried under reduced pressure and purified by silica gel 60 column chromatography. Compounds were successively eluted with acetone-hexane (2:1, v/v), acetone and methanol. The fractions containing the target products were further purified by HPLC using the same method mentioned above, yielding 5.6 mg of quercetin-7-O-β-D-glucoside (3) and 2.5 mg of quercetin-3-O-β-D-glucoside (4). The purified products were dissolved in DMSO-d₆ for NMR spectra.

301 Whole-cell bioconversion of quercetin to quercetin glucosides by E. coli

302 BL21(DE3)/pWZ8 and S. cerevisiae BJ5464/pWZ9

E. coli BL21(DE3)/pWZ8 and S. cerevisiae BJ5464/pWZ9 were grown as described above. After 16 hours, the cells were collected by centrifugation for whole-cell bioconversion. Cells were re-suspended in the reaction buffer, and cell density (OD₆₀₀ value) was determined using a UV-Vis spectrophotometer (Thermo Scientific, Rockford, USA). The whole-cell bioconversion conditions were investigated by testing different pH values (pH 6.0, 6.5, 7.0, 7.5, 8.0, and 8.5), temperatures (25, 30, 35, 40, and 45 °C), cell densities (OD₆₀₀ 2, 4, 6, 8, 10, and 12), reaction times (1, 3, 5, and 7 h) and substrate concentration (0.4, 0.8, 1.6, 3.2, and 5.0 mM). After the optimal conditions were determined, the whole-cell biotransformation experiment was performed in a 1-L reaction system.

Results

Amplification and sequence analysis of a putative GT gene from B. bassiana

The genome of *B. bassiana* ATCC 7159 has been previously sequenced by our group. Searching the genome sequence revealed the presence of a glucosyltransferase (GT) gene that is putatively involved in the commonly observed glucosylation and 4'-O-methylglucosylation by this strain. We named this gene as *Bbgt* (GenBank accession number MW736592). It was predicted that this 1,386-bp gene contains no introns, thus can be directly amplified from the genome of *B. bassiana* ATCC 7159. BLAST analysis indicated that the deduced protein of this gene was homologous to a variety of GTs. A phylogenetic tree was established based on the sequences of BbGT and 19 GTs from other organisms (Fig. 2). The phylogenetic tree mainly divided those 20 GTs into three classes: sterol GTs, flavonoid GTs, and terpene GTs. BbGT is more closely related to sterol GTs and flavonoid GTs than terpene GTs, suggesting that this enzyme is likely a flexible GT which can add the sugar moiety to different sugar-acceptor substrates.

Heterologous expression and purification of BbGT from E. coli BL21(DE3)

The gene was amplified from the genomic DNA of *B. bassiana*, and it was ligated to pET28a to yield the corresponding expression plasmid, pWZ8 (pET28a-*Bbgt*). The plasmid was expressed in *E. coli* BL21(DE3) with IPTG induction. The N-His₆-tagged BbGT was purified through Ni-NTA column chromatography to homogeneity. The purified enzyme was analyzed by SDS-PAGE. As shown in Fig. 3a, BbGT (~50.4 kDa) was successfully expressed and purified from *E. coli* BL21(DE3)/pWZ8. The isolation yield of BbGT was 13.6 mg/L.

In vitro functional characterization of BbGT

Since the phylogenetic analysis suggested that BbGT is more related to sterol GTs and flavonoids GTs, we first tested whether it can glycosylate the sterol resibufogenin, in the presence of UDP-glucose. However, no products were formed (Fig. S1). We next tested the flavonoid quercetin as a potential substrate. HPLC analysis (Fig. 3b) showed that six more polar

products were formed. ESI-MS spectra (Fig. 3c) of **1-6** showed the corresponding quasimolecular ion [M-H]⁻ at *m/z* 624.9, 462.8, 462.9, 462.9, 462.9, and 462.9, respectively. Therefore, products **2-6** have the same molecular weight of 464, which is 162 mass units larger than the substrate quercetin, indicating that a glucose moiety was added to different hydroxyl groups of quercetin. These products were deduced to be quercetin monoglucosides. Since quercetin has five free phenolic hydroxyl groups, we propose that the glucose moiety was introduced to each of these hydroxyl groups to generate the five monoglucosides (Fig. 1). The molecular weight of **1** was found to be 626, which is 324 mass units larger than the substrate or 162 units larger than **2-6**, suggesting that two glucose moieties were added to quercetin to form a diglucoside. Thus, its function was characterized as a UDP-glucosyltransferase.

Broad substrate specificity of BbGT toward sugar acceptor substrates

We next examined whether BbGT can use other substrates. We first tested whether it can use UDP-glucuronic acid since its structure is highly similar to UDP-glucose. However, no products were formed from quercetin (data not shown), indicating that BbGT is a specific UDP-glucosyltransferase that only recognizes UDP-glucose as a sugar donor.

The substrate specificity of BbGT toward sugar acceptor substrates was also investigated. Several substrates, including curcumin, resveratrol, zearalenone, tetracycline, and indigoidine were incubated with BbGT in the presence of UDP-glucose. HPLC analysis showed that compared to the negative control (trace i, Fig. 4a), BbGT generated two more polar products C1 and C2 (trace ii), at 19.8 and 23.9 min respectively, from curcumin. The two products showed the UV spectra (Figs. S2a and S2b) similar to that of the substrate. The ESI-MS spectra (Figs. S3a and S3b) of the two products showed the [M-H] ion peaks at m/z 691.0 and 528.8, indicating that their molecular weights are 692 Da and 530 Da. These are consistent with a diglucoside and a monoglucoside of curcumin, whose molecular weight is 368 Da. This result indicated that BbGT can take curcumin as the substrate for glucosylations.

When the macrolactone zearalenone was used as the substrate, two more polar products **Z1** and **Z2** at 18.5 and 22.5 min were detected by HPLC (Fig. 4b). Similarly, two products **R1** and **R2** appeared at 12.2 and 13.8 min when BbGT reacted with resveratrol (Fig. 4c). All products showed the similar UV spectra (Figs. S2c-f) to the substrates. The ESI-MS spectra (Figs. S3c and S3d) of **Z1** and **Z2** showed a [M-H] ion peak at m/z 479.0 and 478.9, respectively, indicating that their molecular weights are 480 Da, which is consistent with the addition of a glucose moiety to zearalenone. The ESI-MS spectra (Figs. S3e and S3f) of **R1** and **R2** showed a [M-H] ion peak at m/z 389.1 and 389.0, respectively. Their molecular weights were thus determined to be 390 Da, suggesting that they are monoglucosylated products of resveratrol. For tetracycline and indigoidine, no products were found (data not shown), indicating that these two substrates were not taken by BbGT as the sugar acceptor substrate.

The basis for the broad substrate specificity of BbGT was also investigated using homology modeling. The model (Fig. 5a) suggests the BbGT adopts a GT-B fold, with the C-terminal domain binding the sugar donor and the N-terminal domain binding the quercetin acceptor (Chang et al. 2011; Erb et al. 2009; Schmid et al. 2016). Residues important for binding UDP-glucose (Thr280, D374) and the active site histidine base (His20) in the flavonoid glucosyltransferase from *Vitis vinifera* (which uses UDP-glucose donor and quercetin acceptor molecules) (Offen et al. 2006) are conserved in the homology model of BbGT (Thr300, D390 and His31, respectively). Hydrophobic residues in BbGT are positioned on one face of the acceptor binding pocket (Fig. 5b), which is also peppered with side chains capable of interacting with the hydroxyl groups of quercetin (Figs. 5c-e). The acceptor pocket is wide and composed of numerous loops, the movement of which could help to explain the promiscuity observed in substrate selection by BbGT. Figures 5c-e show that the quercetin molecule can be positioned in the pocket in multiple conformations, each placing a different hydroxyl group of quercetin in line for attack of the UDP glucose donor, presumably using the network of available

hydrogen bond donors/acceptors in the active site to reposition the acceptor molecule. The open active site (Dai et al. 2021; Offen et al. 2006), the presence of numerous loops (Schmid et al. 2016), strategic location of hydrogen-bonding acceptors/donors in a relatively hydrophobic pocket (Gatti-Lafranconi and Hollfelder 2013), and predicted conformational changes upon binding of the substrates (Hu et al. 2003; Offen et al. 2006; Schmid et al. 2016) likely all contribute to the observed promiscuity in product specificity.

Determination of the optimal in vitro reaction conditions of BbGT

Quantification of quercetin conversion showed that BbGT has the highest glucosylation activity at 35 °C (Fig. 6a). The glucosylation activity of BbGT increased significantly by 31.50% when the temperature increased from 10 to 35 °C, but gradually decreased when the reaction temperatures were above 35 °C. Thus, the optimum reaction temperature for BbGT was determined to be 35 °C. The effect of pH on the glucosylation activity of BbGT was then determined. The enzyme was reacted with quercetin at 35 °C but different pH values. The conversion rate of quercetin by BbGT notably increased from 15.6% to 49.9% with the increase of pH from 4.5 to 8.0, and then decreased to 38.9 % at pH 8.5 (Fig. 6b). Therefore, the optimum pH for BbGT is 8.0.

In addition, the effect of various metal ions on the activity of BbGT was also tested. We found that BbGT activity was stimulated by Ca²⁺, Mg²⁺, and Mn²⁺ at the tested concentrations (Fig. 6c). In the presence of these three metal ions, the enzyme activity was 1.38, 1.52, and 1.48-fold higher than that of the control group, respectively. Among them, Mg²⁺ exhibited the strongest stimulating effect, and the conversion rate of quercetin increased by nearly 30% compared to the control. By contrast, when Zn²⁺ was added into the reaction system, the activity of BbGT was inhibited. The conversion rate decreased from 56% to 35.3% (Fig. 6c). Based on these results, the optimal *in vitro* reaction conditions for BbGT are at 35 °C, pH 8.0 with 10 mM of Mg²⁺.

Comparison of the in vivo glucosylation of quercetin by BbGT in different heterologous

expression systems

Quercetin was first incubated with IPTG-induced *E. coli* BL21(DE3)/pWZ8. HPLC analysis showed that *E. coli* BL21(DE3)/pWZ8 was able to convert the substrate (trace i, Fig. 7a) to a major product (trace ii) that corresponds to product 3 in the *in vitro* enzymatic reaction. Besides the retention time, the UV and MS spectra also confirmed that this compound is identical to product 3. Several other product peaks were also detected, but were very minor.

While *E. coli* is the most commonly used microbial host, other microorganisms such as *S. cerevisiae* BJ5464, *P. putida* KT2440 and *P. pastoris* GS115 are also utilized in the biotechnological production of medicinally important natural products (Fidan and Zhan 2015). It is interesting that BbGT expressed in *E. coli* showed different product profiles *in vivo* and *in vitro*. We thus wanted to test additional microbial hosts and see what major products could be formed. When we introduced the plasmid pJR16 (pMiS1-*Bbgt*) into *P. putida* KT2440, the product profile (trace iii, Fig. 7a) was almost the same as in *E. coli*, with 3 as the major product. However, when BbGT was expressed in *S. cerevisiae* BJ5464, incubation of quercetin with this strain yielded 4 as the major product and 3 was not detected at all (trace iv, Fig. 7a). We next introduced BbGT into another yeast strain, *P. pastoris* GS115. HPLC analysis showed that this engineered strain, like the two bacterial strains, converted quercetin to product 3, although with a much lower efficiency (trace v, Fig. 7a). Therefore, products 3 and 4 are the two major glucosylation products of quercetin in the BbGT-harboring microbial hosts. Their UV spectra are shown in Figs. 7b and 7c, which are similar to that of the substrate.

Characterization two major glycosylated products of quercetin in different microbial

434 hosts

We next scaled up the biotransformation of quercetin by E. coli BL21(DE3)/pWZ8 and S. cerevisiae BJ5464/pWZ9. The two major products 3 and 4 were purified from these two strains, respectively, and subjected to NMR analysis (Figs. S4-S13). The proton and carbon signals were assigned based on the 1D and 2D NMR spectra (Table S1). The ¹³C NMR spectra of compounds 3 and 4 both revealed 21 carbon signals. In addition to the signals of quercetin, six additional carbon signals at $\delta_{\rm C}$ 99.9, 77.1, 76.4, 73.1, 69.5, and 60.6 for 3 and $\delta_{\rm C}$ 100.8, 77.6, 76.5, 74.1, 69.9, and 61.0 for 4 were found in the spectra, further suggesting that a glucose moiety was added to one of the hydroxyl groups in quercetin. As shown in the ¹H NMR spectra (Figs. S4 and S8), the anomeric proton signals at δ 5.07 (J = 7.5 Hz), and 5.46 (J = 7.5 Hz) of 3 and 4, respectively, indicated the β-configuration of these two compounds for the glucopyranosyl moiety. The ¹³C NMR spectra showed the glucose anomeric carbon signals at δ 99.9 and 100.8 for compounds 3 and 4, respectively. HMBC spectrum of 3 revealed the correlation of H-1" (δ 5.07, d, J = 7.5 Hz) to C-7 at δ 162.7 (Fig. 7d), which confirmed that **3** has a glucose moiety at C-7. Similarly, H-1" (δ 5.46, d, J=7.5 Hz) of 4 had HMBC correlation to C-3 at δ 133.3, indicating that the glucose moiety was introduced at C-3 (Fig. 7d). Therefore, products 3 and 4 were characterized as quercetin-7-O-β-D-glucoside and quercetin-3-O-β-Dglucoside, respectively. Their chemical shifts determined in this work are consistent with those reported in literature (Lee et al. 2008; Yang et al. 2008).

435

436

437

438

439

440

441

442

443

444

445

446

447

448

449

450

451

452

453

454

455

456

457

458

Optimized production of quercetin-7-O-β-D-glucoside with the engineered *E. coli* BL21(DE3)

We first investigated the effect of different cell concentrations ranging from OD_{600} 2.0 to 12.0 on the formation of quercetin glucosides at 28 °C for 3 hours. To ensure that the substrate is enough for the reactions, 1.3 mM quercetin was used together with 0.11 M glucose. We found that the product titer increased with higher cell concentrations (Fig. 8a). When the OD_{600} value

was 10.0, the conversion rate of quercetin in the biotransformation system reached 43.5%, which was 24.5% higher than the titer at OD_{600} 2.0.

The production of quercetin-7-O-β-D-glucoside at different pH values (pH 6.0-8.5) was determined by HPLC. The highest conversion rate reached 54.0% at pH 7.0 (Fig. 8b), which is 15.6% higher than that at pH 6.0. This is also consistent with the optimum pH for *in vitro* reactions. In order to investigate the impact of temperature on the whole-cell conversion efficiency of quercetin to its glucosides, *E. coli* BL21(DE3)/pWZ8 cells (OD₆₀₀ 10.0) were incubated in 200 mM phosphate buffer (pH 7.0) at different temperatures ranging from 25 to 45 °C. The data showed that the increase in the reaction temperature could effectively improve the conversion of quercetin to quercetin-7-O-β-D-glucoside. The highest conversion rate reached 43.0% at 35 °C (Fig. 8c).

We next determined how the bioconversion time affects the conversion rate of quercetin in the engineered *E. coli* strain. To this end, we conducted a time course analysis for the conversion of 10 mM quercetin to it glucosides by BbGT-expressing *E. coli* BL21(DE3) strain (OD₆₀₀ 10.0) at 35 °C in 200 mM phosphate buffer (pH 7.0). The reaction was sampled at 1, 3, 5, and 7 hours. The conversion rate of quercetin increased from 22.9% to 35.4% in the first 3 hours (Fig. 8d). After that, the increase of the conversion rate slowed down. Therefore, the optimum reaction time for the conversion of quercetin to quercetin-7-O-β-D-glucoside by *E. coli* BL21(DE3)/pWZ8 was determined to be 3 hours.

To further optimize the production of quercetin-7-O- β -D-glucoside, we next tested its production from different quercetin concentrations ranging from 0.4 to 5.0 mM. The reactions were conducted at pH 7.0, OD₆₀₀ 10, and 35 °C for 3 hours. When the substrate concentration increased from 0.4 mM to 0.8 mM, the conversion of quercetin to its glucosides also increased from 71.8% to 79.8%. However, when the concentration of quercetin was further increased to 1.6 mM, the conversion rate dropped to 44.5% (Fig. 8e). Based on the productivity of quercetin-

7-O- β -D-glucoside, 0.8 mM was deemed to be the optimal substrate concentration. We then scaled up the reaction to 1 L. The titer of quercetin-7-O- β -D-glucoside reached 0.34 \pm 0.02 mM (equivalent to 158 \pm 8 mg/L) from a total of 0.83 mM (equivalent to 250 mg/L) of quercetin in 24 hours.

Optimized production of quercetin-3-O-β-D-glucoside with the engineered S. cerevisiae

BJ5464

We first investigated the effect of different cell concentrations ranging from OD_{600} 2.5 to 15.0 on the conversion of quercetin to quercetin-3-O- β -D-glucoside by *S. cerevisiae* BJ5464/pWZ9 cells at 35 °C for 3 hours. To ensure that the substrate is enough for the reactions, 0.8 mM quercetin was used together with 0.11 M glucose. We found that the product titer increased with increasing cell concentrations (Fig 9a). When the OD_{600} value was 7.5, the conversion rate of quercetin reached 53.8%, which was 24.4% higher than the titer at OD_{600} 2.5.

In order to investigate the impact of pH on the whole-cell conversion efficiency of quercetin, *S. cerevisiae* BJ5464/pWZ9 cells (OD₆₀₀ 7.5) were incubated with the substrate in 200 mM phosphate buffer (pH 6.5-8.5) at 28 °C for 12 hours. At pH 6.5, the conversion rate was extremely low. With the increasing pH values, the conversion rate also increased apparently. The highest conversion rate reached 55.1% at pH 8 (Fig. 9b), which is higher than the optimal pH for *E. coli* BL21(DE3)/pWZ8 cells. The production of quercetin-3-O-β-D-glucoside at different temperatures (20-40 °C) was also investigated. The highest conversion rate reached 59.8% at 35 °C (Fig. 9c), which is 31.9% higher than that at 20 °C.

We then examined how the reaction time affects the conversion of quercetin in the engineered yeast. To this end, we conducted a time course analysis for the conversion of 0.8 mM quercetin to quercetin-3-O- β -D-glucoside by BbGT-expressing *S. cerevisiae* BJ5464 strain (OD₆₀₀ 7.5) at 35 °C in 200 mM phosphate buffer (pH 8.0). The reaction was sampled at 3, 6,

9, 12, and 15 hours, and the product was quantified by HPLC. The production of quercetin-3-O-β-D-glucoside increased apparently from 3 to 12 hours (Fig. 9d), and the conversion rate was increased from 6.3% to 45.5%. After 12 hours, the increase of the conversion rate slowed down. Therefore, the optimum reaction time for this reaction using *S. cerevisiae* BJ5464/pWZ9 is 12 hours under the tested conditions.

To find out the optimal substrate concentration, we incubated the strain with different quercetin concentrations ranging from 0.2 to 3.2 mM. The reactions were conducted at pH 8.0, OD₆₀₀ 7.5, and 35 °C for 12 hours. When the substrate concentration increased from 0.2 mM to 0.4 mM, the conversion rates of quercetin to quercetin-3-O- β -D-glucoside were similar and both were higher than 60%. However, when the concentration of quercetin was 0.8 mM, the conversion rate dropped to 39.9% (Fig. 9e). Based on the productivity of glucosylated quercetin, 0.4 mM quercetin was selected for scaled-up reaction. The titer of quercetin-3-O- β -D-glucoside in a 1-L reaction system was 0.22 \pm 0.02 mM (equivalent to 99 \pm 8 mg/L) from a total of 0.41 mM (equivalent to 125 mg/L) of quercetin in 12 hours. As a result, *S. cerevisiae* BJ5464/pWZ9 represents a promising strain for cost-effective production of quercetin-3-O- β -D-glucoside.

Discussion

B. bassiana has attracted a lot of attention because of its ability to perform diverse enzymatic modifications (including glycosylation) of exogenous substrates (Sordon et al. 2019; Strugała et al. 2017; Zeng et al. 2010). We previously used this strain to synthesize curcumin-8'-O-4"-O-methyl-β-D-glucopyranoside from curcumin. The water solubility of this glycoside is 39,000-fold higher than the substrate (Zeng et al. 2010). In this study, we discovered and cloned a versatile GT BbGT from *B. bassiana* ATCC 7159, which can glycosylate the representative flavonoid quercetin in a highly flexible way. In addition, BbGT showed a flexible substrate

specificity toward sugar acceptor substrates, and can glycosylate resveratrol, curcumin and zearalenone into their glucosides.

The optimum reaction temperature for BbGT was found to be 35 °C in phosphate buffer. It is similar to those reported GTs, namely BsGT1, BsGT2, and BsGT110 (40 °C) from *Bacillus subtilis* (Cheng et al. 2019; Chiang et al. 2018) and UGT74AN3 from *Catharanthus roseus* (40 °C) (Wen et al. 2020). The optimum pH for BbGT was found to be 8.0, which is the same as the optimum pH for three recently reported UDP-glucosyltransferases, including BsGT1, BsGT2 from *B. subtilis* and UGT74AC1 from *Siraitia grosvenorii*, and three ApUFGTs from *Andrographis paniculata* (Cheng et al. 2019; Li et al. 2019; Mu et al. 2020). However, this value is higher than that of BsGT110 from *B. subtilis* (pH 7.0) (Chiang et al. 2018). Temperature and pH have significant impacts on the conversion of quercetin into quercetin glucosides, and these results indicate that UDP-glucosyltransferases are more active in mild conditions.

Metal ions play an important role in the biological function of many enzymes (Riordan 1977; Sigel and Pyle 2007). Furthermore, previous studies on UGTs showed that Mg²⁺, Ba²⁺, and Ca²⁺ ions exhibited a consistently positive effect on the enzymatic activity (Mu et al. 2020). Therefore, we also tested the effect of metal ions (Ca²⁺, Mg²⁺, Mn²⁺, and Zn²⁺) on the activity of BbGT. Among the four tested metal ions, Ca²⁺, Mg²⁺ and Mn²⁺ can stimulate the activity of BbGT. This result is in accordance with the previous report that GTs can utilize divalent metal ions such as Mn²⁺ and Mg²⁺ as enzyme reaction cofactors (Chiang et al. 2018). Li et al. also found that Ca²⁺ enhanced the activity of the GT from *Bacillus circulans* because of an additional calcium-binding site in the enzyme structure (Li et al. 2013). By contrast, Zn²⁺ showed inhibition to the enzymatic activity of BbGT. This is similar to the previous finding where UGT74AC1 from *S. grosvenorii* was strongly inhibited by Zn²⁺ (Mu et al. 2020). Researchers have previously found that Zn²⁺ is a reversible and competitive inhibitor within the active site

of the glucosyltransferase at the fructose subsite (Devulapalle and Mooser 1994), which may explain its inhibition effect on BbGT enzyme reported here.

Plants and microorganisms are known to contain GTs that can catalyze the glycosylation of flavonoids. Because the 3- and 7-OH are commonly present in many flavonoids, 3-O-GT and 7-O-GT are the most widely investigated (Cao et al. 2015; Yang et al. 2018). However, most GTs have strict regional selectivity and substrate specificity (Cartwright et al. 2008; Overwin et al. 2015). BbGT identified in this work was found to be a highly flexible enzyme in terms of the glucosylation position. The homology model of BbGT (Fig. 5) showed that the cavity is large enough for quercetin to easily rotate and expose different hydroxyl groups to the sugar donor for glucosylations, which explains the production of various quercetin monoglucosides. It is also a versatile enzyme as it can accept a variety of aromatic structures and convert them into monoglucosides and even diglucosides.

There are two novel phenomena observed for BbGT. First, this fungal UGT showed different product profiles *in vitro* and *in vivo*, when quercetin was used as a substrate. The enzyme generated six quercetin glucosides in the *in vitro* reactions, while it produced quercetin-7-O-β-D-glucoside as the dominant product in *E. coli*. No diglucoside of quercetin was detected in *vivo*. The different product profiles between *in vitro* and *in vivo* are likely due to the availability of UDP-glucose and interference of other endogenous proteins in the host. Second, different *in vivo* systems also showed different product profiles. *E. coli*, *P. putida* and *P. pastoris* had similar products, but *S. cerevisiae* produced quercetin-3-O-β-D-glucoside as the major product. The different product profiles may be indicative of host-dependent changes in the BbGT substrate specificity using host-specific post-translational modifications or oligomerization patterns and/or protein regulators. Future work on identification of the post-translational modification patterns observed in different hosts could provide some clues into this interesting phenomenon.

Whole-cell biotransformation eliminates the need of cell disruption and enzyme purification, and can provide UDP-glucose in situ for the glucosylation of quercetin, thus representing a better way to produce quercetin glucosides than in vitro enzymatic reactions. Meanwhile, process optimization is a topic of central importance in industrial production processes. The temperature and pH play critical roles in product formation during whole-cell biotransformation. The optimum temperature for whole-cell bioconversion is the same as the purified enzyme. However, the optimum pH for whole-cell bioconversion with engineered E. coli is 7, which is lower than that in vitro reactions. In the 1-L reaction system, the titer of quercetin-7-O- β -D-glucoside in engineered E. coli strain was 158 \pm 8 mg/L from 250 mg/L quercetin in 24 hours. With the engineered S. cerevisiae BJ5464/pWZ9 strain, the optimum temperature and pH were same as those for the purified enzyme. The titer of quercetin-3-O-β-D-glucoside in shaker flasks was 99 ± 8 mg/L from 125 mg/L quercetin in 12 hours. Lim used the E. coli BL21 culture expressing UGT73B3 as the whole-cell biocatalyst to produce quercetin-3-O-β-D-glucoside, and the titer was around 100 mg/L after 20 hours under fermenter-scale condition (Lim et al. 2004). Xia expressed UGT73B3 in E. coli MEC367 with 30 g/L glucose as the sole carbon source, and the production titer of quercetin-3-O-β-Dglucoside reached 3.9 g/L in 56 hours in controlled bioreactors (Xia and Eiteman 2017). To improve the production of these glucosides by BbGT, the expression of BbGT may be enhanced through synthetic biology and metabolic engineering approaches such as codon optimization of Bbgt and increased production of UDP-glucose in the host. It also was reported that bioreactors can provide better oxygen transfer rates than shaker flaks (Xia and Eiteman 2017), which can further increase the production of these glucosides.

581

582

583

584

585

586

587

588

589

590

591

592

593

594

595

596

597

598

599

600

601

602

603

604

605

In summary, this work identified a highly flexible and versatile GT for glucosylation of a variety of natural products. The enzyme showed different product profiles from quercetin *in vitro* and in various microbial systems. This work also provides two engineered strains for

specific and efficient production of quercetin-7-O-β-D-glucoside and quercetin-3-O-β-D-606 glucoside, by using BbGT in different microbial hosts and optimizing the corresponding 607 reaction conditions. 608 609 **Author contributions** JR, WT and JZ conceived and designed research. JR, WT, CDB, OP, MWM, AP, BW, SEH, and LPS conducted experiments. JR, WT, JH, and JZ analyzed 610 data. JR, WT and JZ wrote the manuscript. All authors read and approved the manuscript. 611 612 **Funding information** This work was supported by the National Science Foundation Award CBET-2044558. The Bruker Avance III HD Ascend-500 NMR instrument used in this 613 614 research was funded by the National Science Foundation Award CHE-1429195. 615 **Compliance with ethical standards Conflict of interest** The authors declare that they have no conflict of interest. 616 **Ethical approval** This article does not contain any studies with human participants or 617 animals performed by any of the authors. 618 Data availability statement All data generated or analyzed during this study are included in 619 this published article (and its supplementary information files). 620 References 621 Anuradha R, Sukumar D (2013) In vitro anti-inflammatory compound quercimeritrin isolated 622 from tithonia diversifolia flowers by hrbc membrane stabilization. World J Pharm Res 623 3(1):426-431. 624 Cai X, Fang Z, Dou J, Yu A, Zhai G (2013) Bioavailability of quercetin: problems and promises. 625 Curr Med Chem 20(20):2572–2582. https://doi.org/10.2174/09298673113209990120 626 Cao H, Chen X, Jassbi AR, Xiao J (2015) Microbial biotransformation of bioactive flavonoids. 627 Biotechnol Adv 33(1):214–223. https://doi.org/10.1016/j.biotechadv.2014.10.012 628

629	Caputi L, Lim EK, Bowles DJ (2008) Discovery of new biocatalysts for the glycosy.	lation of
630	terpenoid scaffolds. Chemistry 14(22):665	6–6662.
631	https://doi.org/10.1002/chem.200800548	
632	Cartwright AM, Lim E-K, Kleanthous C, Bowles DJ (2008) A kinetic analysis of region	specific
633	glucosylation by two glycosyltransferases of Arabidopsis thaliana: domain swa	pping to
634	introduce new activities. J Biol Chem 283(23):15724	-15731.
635	https://doi.org/10.1074/jbc.M801983200	
636	Chang A, Singh S, Phillips GN, Jr., Thorson JS (2011) Glycosyltransferase structural	biology
637	and its role in the design of catalysts for glycosylation. Curr Opin Bio	otechnol
638	22(6):800-808. https://doi.org/10.1016/j.copbio.2011.04.013	
639	Chang T-S, Wu J-Y, Wang T-Y, Wu K-Y, Chiang C-M (2018) Uridine diphosphate-de	ependent
640	glycosyltransferases from Bacillus subtilis ATCC 6633 catalyze the 15-O-glyco	sylation
641	of ganoderic acid A. Int J Mol Sci 19(11):3469. https://doi.org/10.3390/ijms19	113469
642	Chen Q, Li P, Xu Y, Li Y, Tang B (2015) Isoquercitrin inhibits the progression of pa	ncreatic
643	cancer in vivo and in vitro by regulating opioid receptors and the mitogen-a	activated
644	protein kinase signalling pathway. Oncol Rep 33(2):8	40-848.
645	https://doi.org/10.3892/or.2014.3626	
646	Cheng Y, Zhang J, Shao Y, Xu Y, Ge H, Yu B, Wang W (2019) Enzyme-c	atalyzed
647	glycosylation of curcumin and its analogues by glycosyltransferases from	Bacillus
648	subtilis ATCC 6633. Catalysts 9(9):734. https://doi.org/10.3390/catal9090734	
649	Chiang C-M, Wang T-Y, Yang S-Y, Wu J-Y, Chang T-S (2018) Production of new iso	oflavone
650	glucosides from glycosylation of 8-hydroxydaidzein by glycosyltransfera	se from
651	Bacillus subtilis ATCC 6633. Catalysts 8(9):387. https://doi.org/10.3390/catal8	8090387
652	Cregg JM, Russell KA (1998) Transformation <i>Pichia</i> protocols. Springer, pp 27–39.	

Dai L, Li J, Yang J, Zhu Y, Men Y, Zeng Y, Cai Y, Dong C, Dai Z, Zhang X (2018) Use of a 653 654 promiscuous glycosyltransferase from *Bacillus subtilis* 168 for the enzymatic synthesis of novel protopanaxatriol-type ginsenosides. J Agric Food Chem 66(4):943-949. 655 https://doi.org/10.1021/acs.jafc.7b03907 656 Dai L, Qin L, Hu Y, Huang J-w, Hu Z, Min J, Sun Y, Guo R-T (2021) Structural dissection of 657 unnatural ginsenoside-biosynthetic UDP-glycosyltransferase Bs-YjiC from Bacillus 658 subtilis for substrate promiscuity. Biochem Biophys Res Commun 534:73-78. 659 https://doi.org/10.1016/j.bbrc.2020.11.104 660 Day AJ, Mellon F, Barron D, Sarrazin G, Morgan MR, Williamson G (2001) Human 661 metabolism of dietary flavonoids: identification of plasma metabolites of quercetin. 662 Free radic Res 35(6):941–952. https://doi.org/10.1080/10715760100301441 663 Devulapalle KS, Mooser G (1994) Subsite specificity of the active site of glucosyltransferases 664 from Streptococcus sobrinus. J Biol Chem 269(16):11967–11971 665 Dou F, Wang Z, Li G, Dun B (2019) Microbial transformation of flavonoids by Isaria 666 Molecules fumosorosea ACCC 37814. 24(6):1028. 667 https://doi.org/10.3390/molecules24061028 668 Erb A, Weiss H, Härle J, Bechthold A (2009) A bacterial glycosyltransferase gene toolbox: 669 generation applications. Phytochemistry 70(15-16):1812-1821 670 and https://doi.org/10.1016/j.phytochem.2009.05.019 671 Fan J, Chen C, Yu Q, Li Z-G, Gmitter FG (2010) Characterization of three terpenoid 672 673 glycosyltransferase genes in 'Valencia' sweet orange (Citrus sinensis L. Osbeck). Genome 53(10):816–823. https://doi.org/10.1139/G10-068 674 675 Fidan O, Zhan J (2015) Recent advances in engineering yeast for pharmaceutical protein

production. RSC Adv 5(105):86665-86674. https://doi.org/10.1039/C5RA13003D

677	Fidan O, Zhan J (2019) Discovery and engineering of an endophytic <i>Pseudomonas</i> strain from							
678	Taxus chinensis for efficient production of zeaxanthin diglucoside. J Biol Eng 13:66.							
679	https://doi.org/10.1186/s13036-019-0196-x							
680	Gatti-Lafranconi P, Hollfelder F (2013) Flexibility and reactivity in promiscuous enzymes.							
681	ChemBioChem 14(3):285-292. https://doi.org/10.1002/cbic.201200628							
682	Griesser M, Vitzthum F, Fink B, Bellido ML, Raasch C, Munoz-Blanco J, Schwab W (2008)							
683	$\label{eq:multi-substrate} \mbox{Multi-substrate flavonol O-glucosyltransferases from strawberry} \mbox{$(Fragaria \times ananassa)$}$							
684	achene and receptacle. J Exp Bot 59(10):2611–2625. https://doi.org/10.1093/jxb/ern117							
685	Grogan G, Holland H (2000) The biocatalytic reactions of <i>Beauveria</i> spp. J Mol Catal B Enzym							
686	9(1-3):1-32. https://doi.org/10.1016/S1381-1177(99)00080-6							
687	Hirotani M, Kuroda R, Suzuki H, Yoshikawa T (2000) Cloning and expression of UDP-glucose:							
688	flavonoid 7-O-glucosyltransferase from hairy root cultures of Scutellaria baicalensis.							
689	Planta 210(6):1006–1013. https://doi.org/10.1007/PL00008158							
690	Hu Y, Chen L, Ha S, Gross B, Falcone B, Walker D, Mokhtarzadeh M, Walker S (2003) Crystal							
691	structure of the MurG:UDP-GlcNAc complex reveals common structural principles of							
692	a superfamily of glycosyltransferases. Proc Natl Acad Sci USA 100(3):845-849.							
693	https://doi.org/10.1073/pnas.0235749100							
694	Ko JH, Kim BG, Joong-Hoon A (2006) Glycosylation of flavonoids with a glycosyltransferase							
695	from Bacillus cereus. FEMS Microbiol Lett 258(2):263–268.							
696	https://doi.org/10.1111/j.1574-6968.2006.00226.x							
697	Ikeda K, Taguchi R (2010) Highly sensitive localization analysis of gangliosides and sulfatides							
698	including structural isomers in mouse cerebellum sections by combination of laser							
699	microdissection and hydrophilic interaction liquid chromatography/electrospray							
700	ionization mass spectrometry with theoretically expanded multiple reaction monitoring.							
701	Rapid Commun Mass Spectrom 24(20):2957–2965. https://doi.org/10.1002/rcm.4716							

Jiang J-r, Yuan S, Ding J-f, Zhu S-c, Xu H-d, Chen T, Cong X-d, Xu W-p, Ye H, Dai Y-j (2008) 702 Conversion of puerarin into its 7-O-glycoside derivatives by *Microbacterium oxydans* 703 (CGMCC 1788) to improve its water solubility and pharmacokinetic properties. Appl 704 Microbiol Biotechnol 81(4):647–657. https://doi.org/10.1007/s00253-008-1683-z 705 Lairson L, Henrissat B, Davies G, Withers S (2008) Glycosyltransferases: structures, functions, 706 707 and mechanisms. Rev Biochem 77:521-555. Annu https://doi.org/10.1146/annurev.biochem.76.061005.092322 708 Lee S, Park HS, Notsu Y, Ban HS, Kim YP, Ishihara K, Hirasawa N, Jung SH, Lee YS, Lim 709 SS (2008) Effects of hyperin, isoquercitrin and quercetin on lipopolysaccharide-induced 710 nitrite production in rat peritoneal macrophages. Phytother Res 22(11):1552-1556. 711 https://doi.org/10.1002/ptr.2529 712 Legault J, Perron T, Mshvildadze V, Girard-Lalancette K, Perron S, Laprise C, Sirois P, 713 Pichette A (2011) Antioxidant and anti-inflammatory activities of quercetin 7-O-β-D-714 715 glucopyranoside from the leaves of *Brasenia schreberi*. J Med Food 14(10):1127–1134. https://doi.org/10.1089/jmf.2010.0198 716 717 Li C, Ban X, Gu Z, Li Z (2013) Calcium ion contribution to thermostability of cyclodextrin glycosyltransferase is closely related to calcium-binding site CaIII. J Agric Food Chem 718 719 61(37):8836–8841. https://doi.org/10.1021/jf4024273 Li D, Park J-H, Park J-T, Park CS, Park K-H (2004) Biotechnological production of highly 720 721 soluble daidzein glycosides using *Thermotoga maritima* maltosyltransferase. J Agric Food Chem 52(9):2561–2567. https://doi.org/10.1021/jf035109f 722 Li J, Li Z, Li C, Gou J, Zhang Y (2014) Molecular cloning and characterization of an isoflavone 723 7-O-glucosyltransferase from *Pueraria lobata*. Plant Cell Rep 33(7):1173–1185. 724 https://doi.org/10.1007/s00299-014-1606-7 725

- Li Y, Li X-L, Lai C-J-S, Wang R-S, Kang L-P, Ma T, Zhao Z-H, Gao W, Huang L-Q (2019)
- Functional characterization of three flavonoid glycosyltransferases from *Andrographis*
- 728 paniculata. R Soc Open Sci 6(6):190150. https://doi.org/10.1098/rsos.190150
- Liang H, Hu Z, Zhang T, Gong T, Chen J, Zhu P, Li Y, Yang J (2017) Production of a bioactive
- unnatural ginsenoside by metabolically engineered yeasts based on a new UDP-
- 731 glycosyltransferase from *Bacillus subtilis*. Metab Eng 44:60–69.
- 732 https://doi.org/10.1016/j.ymben.2017.07.008
- 733 Lim E-K, Ashford DA, Hou B, Jackson RG, Bowles DJ (2004) Arabidopsis
- glycosyltransferases as biocatalysts in fermentation for regioselective synthesis of
- 735 diverse quercetin glucosides. Biotech Bioeng 87(5):623–631.
- 736 https://doi.org/10.1002/bit.20154
- Lin-Cereghino J, Wong WW, Xiong S, Giang W, Luong LT, Vu J, Johnson SD, Lin-Cereghino
- GP (2005) Condensed protocol for competent cell preparation and transformation of the
- methylotrophic yeast *Pichia pastoris*. Biotechniques 38(1):44–48.
- 740 https://doi.org/10.2144/05381BM04
- 741 Lu Y, Ma B-W, Gao J, Tu L-C, Hu T-Y, Zhou J-W, Liu Y, Tu Y-H, Lin Z-S, Huang L-Q (2020)
- Isolation and characterization of a glycosyltransferase with specific catalytic activity
- towards flavonoids from *Tripterygium wilfordii*. J Asian Nat Prod Res 22(6):537–546.
- 744 https://doi.org/10.1080/10286020.2019.1642330
- Ma B, Zeng J, Shao L, Zhan J (2013) Efficient bioconversion of quercetin into a novel glycoside
- by Streptomyces rimosus subsp. rimosus ATCC 10970. J Biosci Bioeng 115(1):24–26.
- 747 https://doi.org/10.1016/j.jbiosc.2012.07.020
- Makris DP, Rossiter JT (2000) Heat-induced, metal-catalyzed oxidative degradation of
- quercetin and rutin (quercetin 3-O-rhamnosylglucoside) in aqueous model systems. J
- 750 Agric Food Chem 48(9):3830–3838. https://doi.org/10.1021/jf0001280

Matsubara K, Ishihara K, Mizushina Y, Mori M, Nakajima N (2004) Anti-angiogenic activity 751 of quercetin and its derivatives. Lett Drug Des Discov 1(4):329-333. 752 https://doi.org/10.2174/1570180043398533 753 754 Meesapyodsuk D, Balsevich J, Reed DW, Covello PS (2007) Saponin biosynthesis in Saponaria vaccaria. cDNAs encoding β-amyrin synthase and a triterpene carboxylic 755 acid glucosyltransferase. Plant Physiol 143(2):959-969. 756 https://doi.org/10.1104/pp.106.088484 757 Méndez C, Salas JA (2001) Altering the glycosylation pattern of bioactive compounds. Trends 758 Biotechnol 19(11):449–456. https://doi.org/10.1016/S0167-7799(01)01765-6 759 Mfonku NA, Mbah JA, Kodjio N, Gatsing D, Zhan J (2020) Isolation and selective 760 761 glycosylation of antisalmonellal anthraquinones from the stem bark of *Morinda lucida* (Rubiaceae). Phytochem 762 Benth. Lett 37:80-84. 763 https://doi.org/10.1016/j.phytol.2020.04.011 Mu S, Li J, Liu C, Zeng Y, Men Y, Cai Y, Chen N, Ma H, Sun Y (2020) Effective glycosylation 764 of cucurbitacin mediated by UDP-glycosyltransferase UGT74AC1 and molecular 765 766 dynamics exploration of its substrate binding conformations. Catalysts 10(12):1466. https://doi.org/10.3390/catal10121466 767 Offen W, Martinez-Fleites C, Yang M, Kiat-Lim E, Davis BG, Tarling CA, Ford CM, Bowles 768 769 DJ, Davies GJ (2006) Structure of a flavonoid glucosyltransferase reveals the basis for modification. **EMBO** 25(6):1396-1405. 770 plant natural product J https://doi.org/10.1038/sj.emboj.7600970 771 772 Ono E, Fukuchi-Mizutani M, Nakamura N, Fukui Y, Yonekura-Sakakibara K, Yamaguchi M, Nakayama T, Tanaka T, Kusumi T, Tanaka Y (2006) Yellow flowers generated by 773 774 expression of the aurone biosynthetic pathway. Proc Natl Acad Sci USA

103(29):11075–11080. https://doi.org/10.1073/pnas.0604246103

Overwin H, Wray V, Hofer B (2015) Flavonoid glucosylation by non-Leloir 776 777 glycosyltransferases: formation of multiple derivatives of 3,5,7,3',4'pentahydroxyflavane stereoisomers. Appl Microbiol Biotechnol 99(22):9565-9576. 778 779 https://doi.org/10.1007/s00253-015-6760-5 Paulke A, Eckert GP, Schubert-Zsilavecz M, Wurglics M (2012) Isoquercitrin provides better 780 bioavailability than quercetin: comparison of quercetin metabolites in body tissue and 781 782 brain sections after six days administration of isoquercitrin and quercetin. Pharmazie 67(12):991-996 783 Riordan JF (1977) The role of metals in enzyme activity. Ann Clin Lab Sci 7(2):119–129. 784 Schmid J, Heider D, Wendel NJ, Sperl N, Sieber V (2016) Bacterial Glycosyltransferases: 785 challenges and opportunities of a highly diverse enzyme class toward tailoring natural 786 products. Frontiers in Microbiology 7:182. https://doi.org/10.3389/fmicb.2016.00182 787 Sharma LK, Madina BR, Chaturvedi P, Sangwan RS, Tuli R (2007) Molecular cloning and 788 characterization of one member of 3β-hydroxy sterol glucosyltransferase gene family in 789 Biochem 790 Withania somnifera. Arch **Biophys** 460(1):48-55. 791 https://doi.org/10.1016/j.abb.2007.01.024 Sigel RK, Pyle AM (2007) Alternative roles for metal ions in enzyme catalysis and the 792 chemistry. 107(1):97-113. 793 implications for ribozyme Chem Rev https://doi.org/10.1021/cr0502605 794 Sordon S, Popłoński J, Tronina T, Huszcza E (2019) Regioselective O-glycosylation of 795 flavonoids by fungi Beauveria bassiana, Absidia coerulea and Absidia glauca. Bioorg 796 797 Chem 93:102750. https://doi.org/10.1016/j.bioorg.2019.01.046 Strugała P, Tronina T, Huszcza E, Gabrielska J (2017) Bioactivity in vitro of quercetin 798 glycoside obtained in Beauveria bassiana culture and its interaction with liposome 799

membranes. Molecules 22(9):1520. https://doi.org/10.3390/molecules22091520

801	Valentová K, Vrba J, Bancířová M, Ulrichová J, Křen V (2014) Isoquercitrin: pharmacology,								
802	toxicology, and metabolism. Food Chem Toxicol 68:267-282.								
803	https://doi.org/10.1016/j.fct.2014.03.018								
804	Vogt T, Jones P (2000) Glycosyltransferases in plant natural product synthesis: characterization								
805	of a supergene family. Trends Plant Sci 5(9):380-386. https://doi.org/10.1016/S1360								
806	1385(00)01720-9								
807	Wang D-D, Jin Y, Wang C, Kim Y-J, Perez ZEJ, Baek NI, Mathiyalagan R, Markus J, Yang								
808	D-C (2018a) Rare ginsenoside Ia synthesized from F1 by cloning and overexpression								
809	of the UDP-glycosyltransferase gene from Bacillus subtilis: Synthesis, characterization,								
810	and in vitro melanogenesis inhibition activity in BL6B16 cells. J Ginseng Res								
811	42(1):42-49. https://doi.org/10.1016/j.jgr.2016.12.009								
812	Warnecke D, Erdmann R, Fahl A, Hube B, Müller F, Zank T, Zähringer U, Heinz E (1999)								
813	Cloning and functional expression of UGT genes encoding sterol glucosyltransferases								
814	from Saccharomyces cerevisiae, Candida albicans, Pichia pastoris, and Dictyostelium								
815	discoideum. J Biol Chem 274(19):13048-13059.								
816	https://doi.org/10.1074/jbc.274.19.13048								
817	Warnecke DC, Baltrusch M, Buck F, Wolter FP, Heinz E (1997) UDP-glucose:sterol								
818	glucosyltransferase: cloning and functional expression in Escherichia coli. Plant Mol								
819	Biol 35(5):597-603. https://doi.org/10.1023/A:1005806119807								
820	Wen C, Huang W, He M-M, Deng W-L, Yu H-H (2020) Cloning and characterization of a								
821	glycosyltransferase from Catharanthus roseus for glycosylation of cardiotonic steroids								
822	and phenolic compounds. Biotechnol Lett 42(1):135-142.								
823	https://doi.org/10.1007/s10529-019-02756-5								

Wen L, Zhao Y, Jiang Y, Yu L, Zeng X, Yang J, Tian M, Liu H, Yang B (2017) Identification 824 of a flavonoid C-glycoside as potent antioxidant. Free Radic Biol Med 110:92-101. 825 https://doi.org/10.1016/j.freeradbiomed.2017.05.027 826 Xia T, Eiteman MA (2017) Quercetin glucoside production by engineered Escherichia coli. 827 Appl Biochem Biotechnol 182(4):1358–1370. https://doi.org/10.1007/s12010-017-828 2403-x 829 Xu F, Gage D, Zhan J (2015) Efficient production of indigoidine in Escherichia coli. J Ind 830 Microbiol Biotechnol 42(8):1149–1155. https://doi.org/10.1007/s10295-015-1642-5 831 Yang B, Liu H, Yang J, Gupta VK, Jiang Y (2018) New insights on bioactivities and 832 biosynthesis of flavonoid glycosides. Trends Food Sci Technol 79:116-124. 833 https://doi.org/10.1016/j.tifs.2018.07.006 834 Yang Y, Wu T, Yang WX, Aisa HA, Zhang TY, Ito Y (2008) Preparative isolation and 835 836 purification of four flavonoids from Flos Gossypii by high-speed countercurrent Relat chromatography. J. Liq Chromatogr Technol 31(10):1523-1531. 837 https://doi.org/10.1080/10826070802039663 838 Yonekura-Sakakibara K, Hanada K (2011) An evolutionary view of functional diversity in 839 family 1 glycosyltransferases. Plant J 66(1):182–193. https://doi.org/10.1111/j.1365-840 313X.2011.04493.x 841 Yu D, Xu F, Valiente J, Wang S, Zhan J (2013) An indigoidine biosynthetic gene cluster from 842 Streptomyces chromofuscus ATCC 49982 contains an unusual IndB homologue. J Ind 843 844 Microbiol Biotechnol 40(1):159–168. https://doi.org/10.1007/s10295-012-1207-9 Yu D, Xu F, Zhang S, Zhan J (2017) Decoding and reprogramming fungal iterative 845 nonribosomal peptide synthetases. Nat Commun 8(1):1-11.846

https://doi.org/10.1038/ncomms15349

848	Zeng J	I, Yaı	ng N, Li Σ	KM, Sham	i PJ, Zł	nan J (20	10) 4'-0)-Meth	ylglycosy	lation	of curc	umin by
849	Beauveria		bassia	bassiana.		Pr	od	Commun		5(1):77-80.		
850		http	s://doi.org	/10.1177/	1934578	3X10005	00119					
851	Zhan	J,	Gunatila	ka AA	(2006	ba) Mi	crobial	trans	formation	of	amino	o- and
852		hydı	roxyanthra	aquinones	by I	Beauveri	a bass	iana	ATCC	7159.	J Na	t Prod
853		69(1	0):1525–	1527. http:	s://doi.c	org/10.10	21/np06	0339k				
854	Zhan J, Leslie Gunatilaka AA (2006b) Selective 4'-O-methylglycosylation of the pentahydroxy-											
855		flav	onoid qu	ercetin by	у Веаи	veria b	assiana	ATC	C 7159.	Biocat	tal Bio	otransfor
856		24(5	5):396–399	9. https://d	loi.org/1	10.1080/	1024242	06007	92169			
857	Zhao Z	X, W	ang P, Li	M, Wang	Y, Jiai	ng X, Cu	ıi L, Qia	an Y, Z	Zhuang J,	Gao L	., Xia T	(2017)
858		Fun	ctional c	characteriz	ation	of a	new t	ea (C	Camellia	sinens	sis) fl	avonoid
859		glyc	osyltransf	erase.	J	Agric	Foo	d	Chem	65(1	10):207	4–2083.
860		http	s://doi.org	/10.1021/a	acs.jafc.	6b05619	1					
861												
862												
863												
864												
865												
866												
867												
868												
869												
070												
870												

Table 1 Primers and plasmids used in this study.

Gene Name	Primers
Bbgt-NdeI-F	5'-AACATATGTCTCCGTCACGCAGCGAG-3'
Bbgt-PmlI-EcoRI-R	5'-AACACGTGGAATTCTCAATCCATAGCCGCCCACTTG-3'
Bbgt-PmeI-EcoRI-F	5'-AACCGTTTAAACGAATTCATGTCTCCGTCACGCAGCGAG-3'
Bbgt-NotI-HindIII-R	5'-AACCGCGGCCGCAAGCTTTCAATCCATAGCCGCCCACTTG-3'
Plasmid	Description
pJET1.2	Cloning vector with blunt ends
pET28a(+)	E. coli expression vector
YEpADH2p-URA3	Expression vector for S. cerevisiae BJ5464
pPICZB	Expression vector for <i>P. pastoris</i> GS115
pMiS1-mva-ges	Expression vector for P. putida KT2440
pWZ7	Bbgt in pJET1.2
pWZ8	Bbgt in pET28a(+)
pWZ9	Bbgt in YEpADH2p-URA3
pJR10	Bbgt in pJET1.2
pJR14	Bbgt in pPICZB
pJR16	Bbgt in pMiS1

Figure legends

881

Fig. 1 Glucosylation of quercetin by BbGT.

Fig. 2 Phylogenetic analysis of BbGT with other GTs. The numbers following GTs are the 883 numbers of combined guide-tree/HMM iterations. The analyzed GTs include sterol GTs, 884 namely BsUGT489 (Bacillus subtilis, GenBank accession no. WP 003220489, similarity: 18.0 885 %) (Chang et al. 2018), BsUGT398 (B. subtilis, GenBank accession no. WP 003225398, 886 similarity: 22.9 %) (Chang et al. 2018), BsYjiC (B. subtilis, GenBank accession no. 887 NP 389104.1, similarity: 19.6 %) (Dai et al. 2018), UGT109A1 (B. subtilis, GenBank 888 accession no. ASY97769.1, similarity: 18.8 %) (Liang et al. 2017), BsGT1 (B. subtilis, 889 GenBank accession no. ANP92054.1, similarity: 19.6 %) (Wang et al. 2018), AtSGT 890 (Arabidopsis thaliana, GenBank accession no. CAB06082.1, similarity: 19.5 %) (Warnecke et 891 al. 1997), SGTL1 (Withania somnifera, GenBank accession no. ABC96116.1, similarity: 22.4 892 893 %) (Sharma et al. 2007), UGT51C1 (Candida albicans, GenBank accession no. AAD29571.1, similarity: 20.5 %) (Warnecke et al. 1999); flavonoid GTs, namely TwUGT2 (Tripterygium 894 895 wilfordii, GenBank accession no. MK035745.1, similarity: 13.6 %) (Lu et al. 2020), 896 CsUGT73A20 (Camellia sinensis, GenBank accession no. KP682358.1, similarity: 21.1 %) (Zhao et al. 2017), Am4CGT (Antirrhinum majus, GenBank accession no. BAE48239.1, 897 similarity: 22.3 %) (Ono et al. 2006), PIUGT1 (Pueraria lobata, GenBank accession no. 898 AGZ84545.1, similarity: 21.7 %) (Li et al. 2014), UBGT (Scutellaria baicalensis, GenBank 899 accession no. BAA83484.1, similarity: 22.1 %) (Hirotani et al. 2000), FaGT7 (Fragaria 900 ananassa, GenBank accession no. Q2V6J9, similarity: 20.9 %) (Griesser et al. 2008); terpenoid 901 GTs, namely, CsUGT1 (Citrus sinensis, GenBank accession no. GQ221686.1, similarity: 21.5 902 %) (Fan et al. 2010), UGT84B1 (Arabidopsis thaliana, GenBank accession no. At2g23260, 903 904 similarity: 20.9 %) (Caputi et al. 2008), UGT84A4 (A. thaliana, GenBank accession no. At4g15500, similarity: 22.2 %) (Caputi et al. 2008), CsUGT2 (C. sinensis, GenBank accession 905

- no. ACS87991.1, similarity: 21.5 %) (Fan et al. 2010), UGT74M1 (Gypsophila vaccaria,
- 907 GenBank accession no. ABK76266.1, similarity: 20.5 %) (Meesapyodsuk et al. 2007).
- 908 Fig. 3 Expression of BbGT in E. coli and in vitro functional characterization. a SDS-PAGE
- analysis of the purified recombinant BbGT from E. coli BL21(DE3). Lane 1: Purified BbGT;
- Lane 2: Protein ladder. **b** HPLC analysis of the reaction of BbGT with quercetin in the presence
- of UDP-glucose at 350 nm. (i) negative control (without BbGT); (ii) quercetin + BbGT. c-h
- 912 ESI-MS (-) spectra of products 1-6.
- 913 Fig. 4 HPLC analysis of glucosylation of different sugar-acceptor substrates by BbGT. a
- Glucosylation of curcumin (420 nm); **b** Glucosylation of zearalenone (250 nm); **c** glucosylation
- of resveratrol (300 nm). (i) substrate incubated with the reaction buffer without BbGT; (ii)
- substrate incubated with the reaction buffer with BbGT.
- 917 Fig. 5 Homology modeling of the BbGT. a The structure of BbGT was predicted using
- 918 homology modeling. The model shows a GT-B fold where the C-terminal domain encompasses
- 919 the sugar donor binding site (gray) and the N-terminal domain houses the acceptor binding site
- 920 (teal) with the active site formulated at the interface. A quercetin molecule (magenta) and UDP-
- 2-deoxy-2-fluoro glucose (green) are shown based on their positions in the 2C9Z and 2C1Z
- structures, respectively. **b** The hydrophobic character of the quercetin binding pocket is shown
- as red (high hydrophobicity) and white (low hydrophobicity). In c-e, the quercetin molecule
- 924 (cyan with oxygen atoms colored yellow) was placed into the active site to position three of the
- 925 possible nucleophilic hydroxyl groups within 4-5 Å of C-1 of the donor sugar. Potential
- 926 hydrogen bond donors/acceptors (purple) are present throughout the mostly hydrophobic
- 927 pocket.
- 928 Fig. 6 Determination of the optimum *in vitro* reaction conditions for BbGT. a Effect of reaction
- 929 temperature on the BbGT glucosylation activity. **b** Effect of reaction pH on the BbGT

- glucosylation activity. **c** Effect of metal ions on the BbGT glucosylation activity. Data are presented as the mean ± SD from three independent experiments.
- **Fig. 7** HPLC analysis of glucosylation of quercetin by BbGT in different heterologous expression systems. **a** HPLC traces (350 nm) of the standard of quercetin and biotransformation product profiles from different engineered strains. (i) commercial standard of quercetin; (ii) quercetin + *E. coli* BL21(DE3)/pWZ8; (iii) quercetin + *P. putida* KT2440/pJR16; (iv) quercetin + *S. cerevisiae* BJ5464/pWZ9; (v) quercetin + *P. pastoris* GS115/pJR14. Asterisked peaks in trace iv are the metabolites from the host. **b** UV spectra comparison of the substrate and product **3. c** UV spectra comparison of the substrate and product **4. d** Selected HMBC correlations for

products 3 and 4.

- **Fig. 8** Optimization of the glucosylation of quercetin by *E. coli* BL21(DE3)/pWZ8. **a** Effect of cell density on quercetin glucosylation by *E. coli* BL21(DE3)/pWZ8. **b** Effect of reaction pH on quercetin glucosylation by *E. coli* BL21(DE3)/pWZ8. **c** Effect of temperature on quercetin glucosylation by *E. coli* BL21(DE3)/pWZ8. **d** Effect of reaction time on quercetin glucosylation by *E. coli* BL21(DE3)/pWZ8. **e** Effect of substrate concentration on quercetin glucosylation by *E. coli* BL21(DE3)/pWZ8. Data are presented as the mean ± SD from three independent experiments.
 - **Fig. 9** Optimization of the whole-cell conversion of BbGT to quercetin-3-O-β-D-glucoside by *S. cerevisiae* BJ5464/pWZ9. **a** Effect of cell density on the production of quercetin-3-O-β-D-glucoside by *S. cerevisiae* BJ5464/pWZ9. **b** Effect of reaction pH on the production of quercetin-3-O-β-D-glucoside by *S. cerevisiae* BJ5464/pWZ9. **c** Effect of temperature on the production of quercetin-3-O-β-D-glucoside by *S. cerevisiae* BJ5464/pWZ9. **d** Effect of reaction time on the production of quercetin-3-O-β-D-glucoside by *S. cerevisiae* BJ5464/pWZ9. **e** Effect of substrate concentration on the production of quercetin-3-O-β-D-glucoside by *S. cerevisiae* BJ5464/pWZ9. Data are presented as the mean ± SD from three independent experiments.

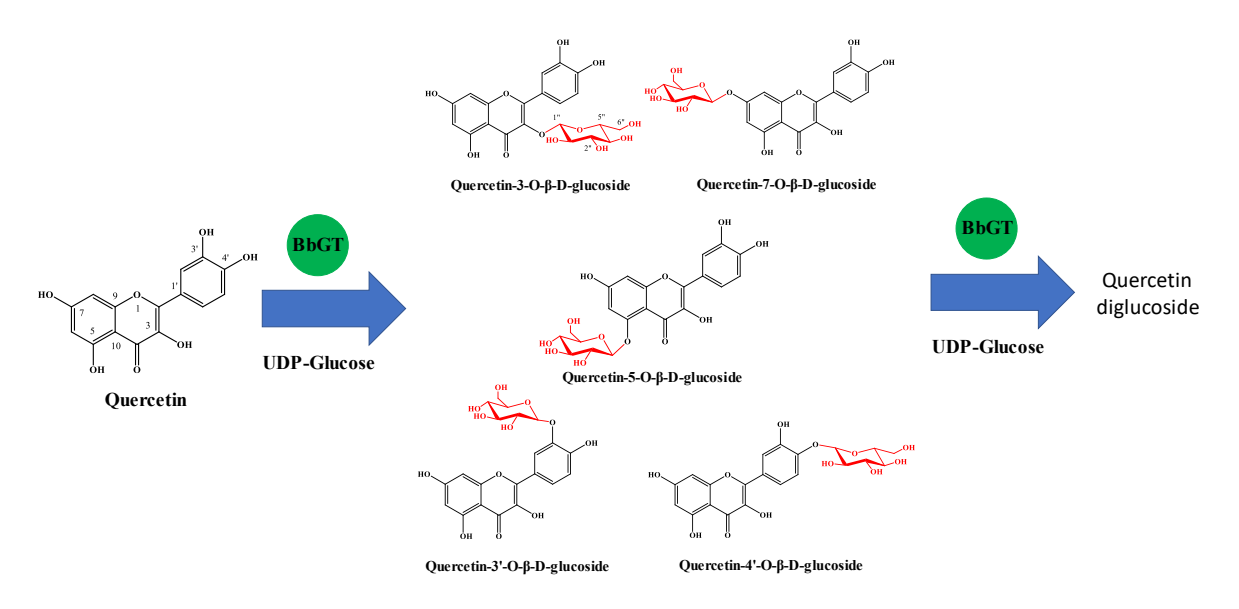
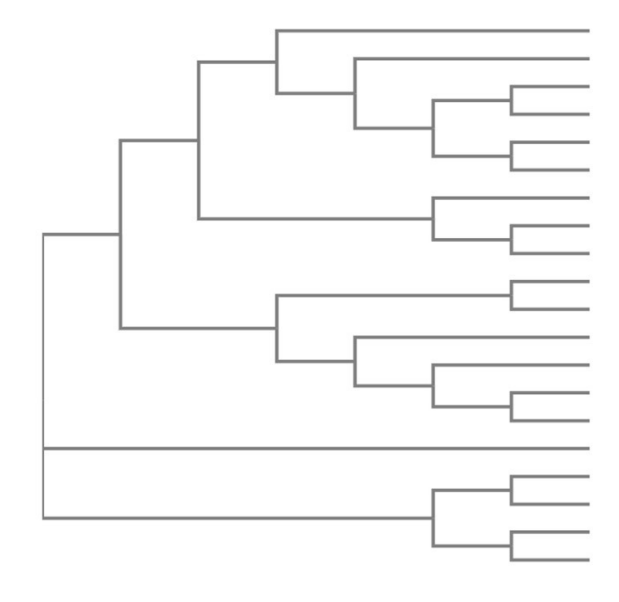


Fig. 1

979



BbGT 0.42126 BsUGT398 0.30626 BsYjiC 0.05826 BsGT1 0.06007 BsUGT489 0.03546 UGT109A1 0.04437 UGT51C1 0.35058 AtSGT 0.26865 SGTL1 0.25408 Am4CGT 0.30406 PIUGT1 0.28214 TwUGT2 0.34502 UBGT 0.24119 CsUGT73A20 0.20586 FaGT7 0.21678 UGT74M1 0.34109 CsUGT1 0.00199 CsUGT2 0.00131 UGT84B1 0.26428 UGT84A4 0.2832

Flavonoid GTs

Sterol GTs

Terpenoid GTs

981 Fig. 2

982

980

983

984

985

986

987

988

989

990



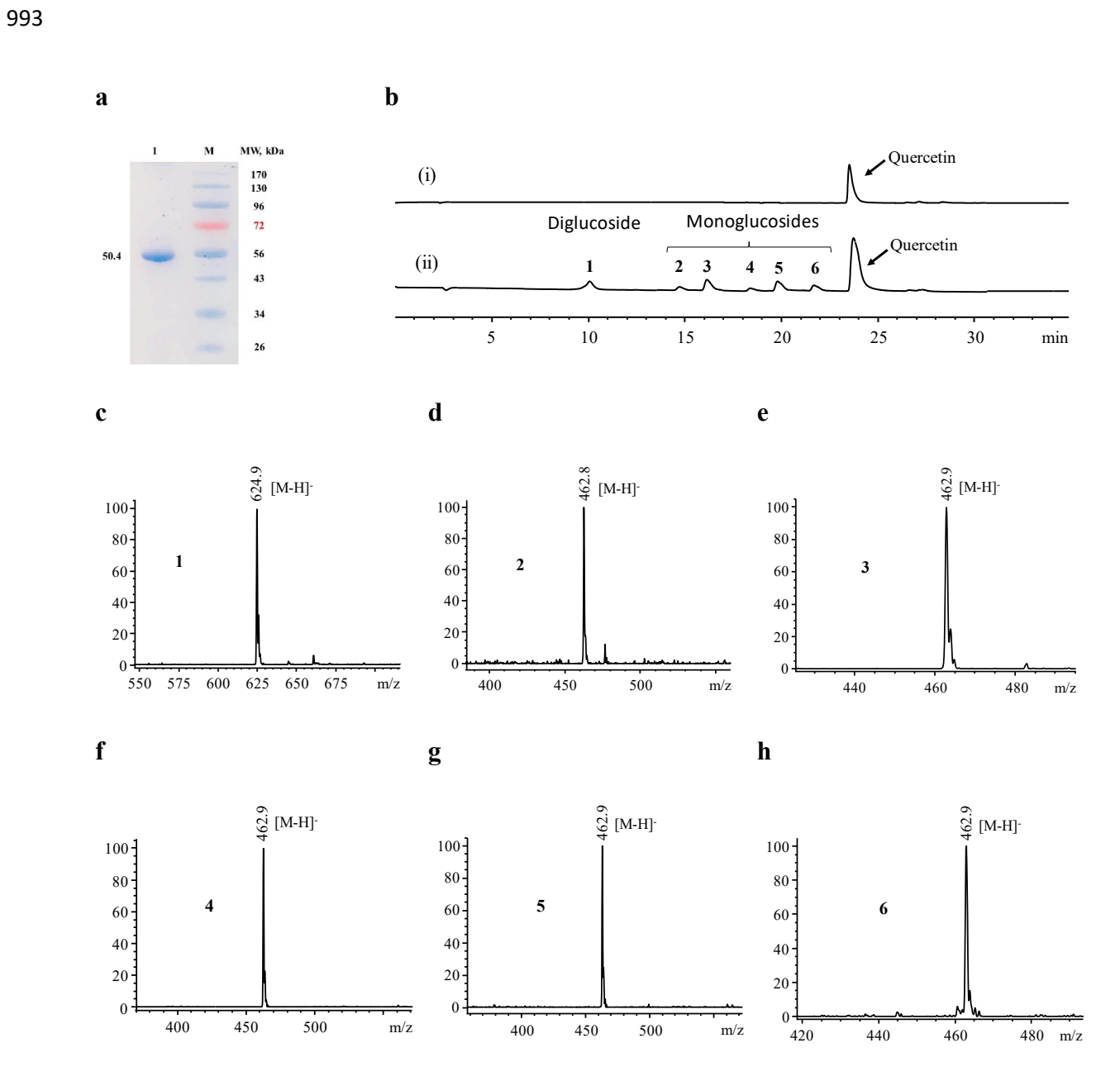
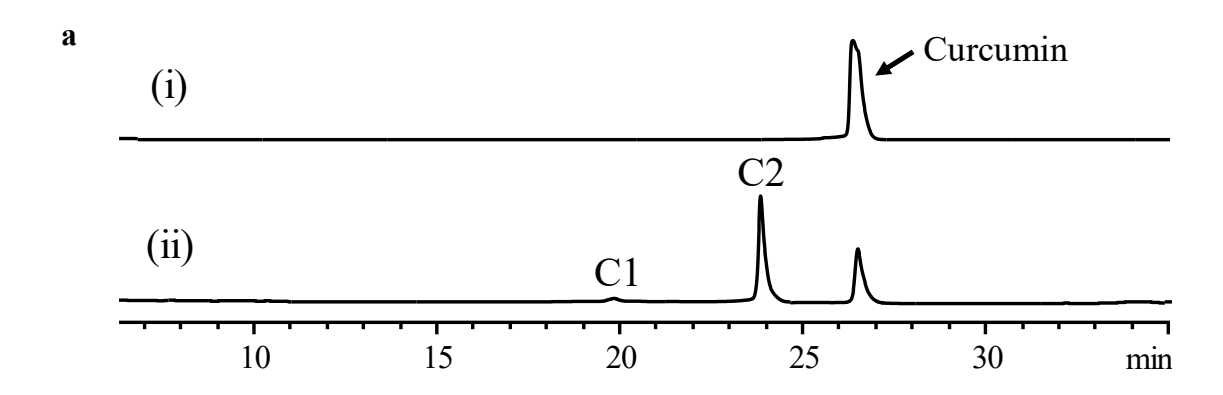
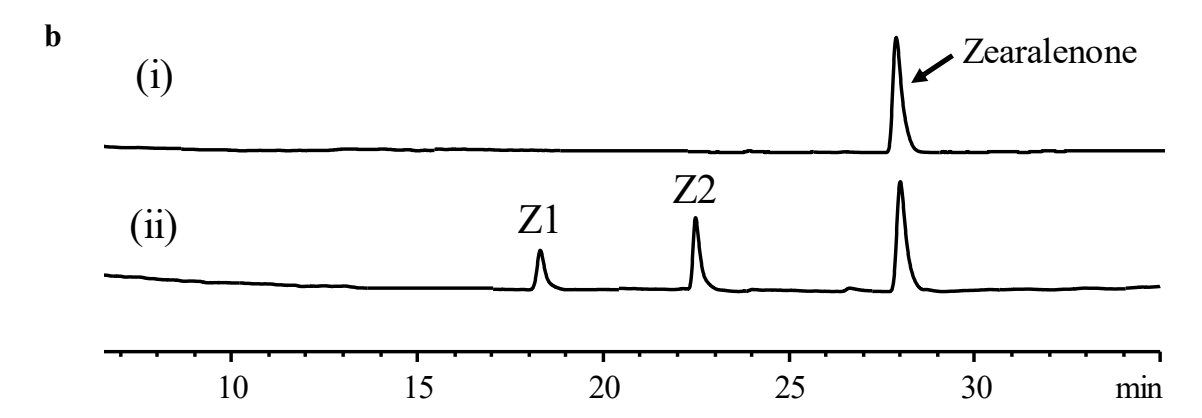
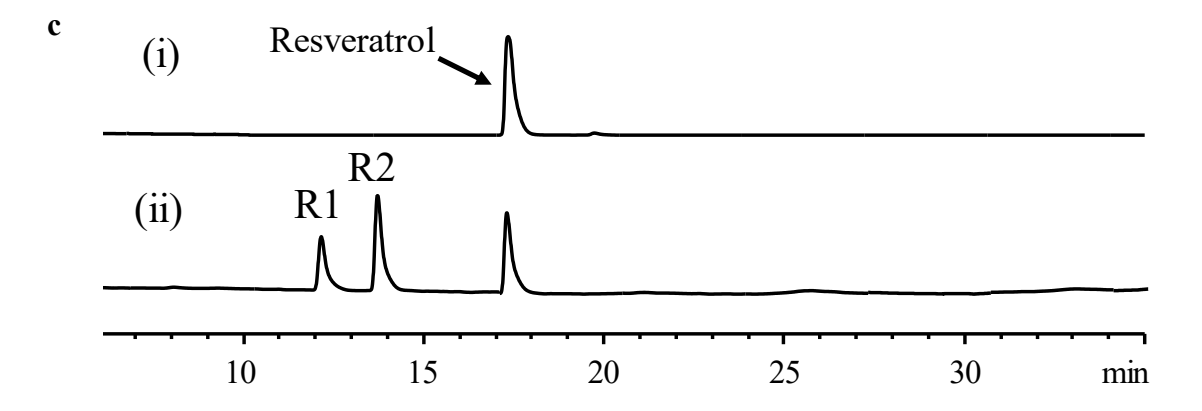


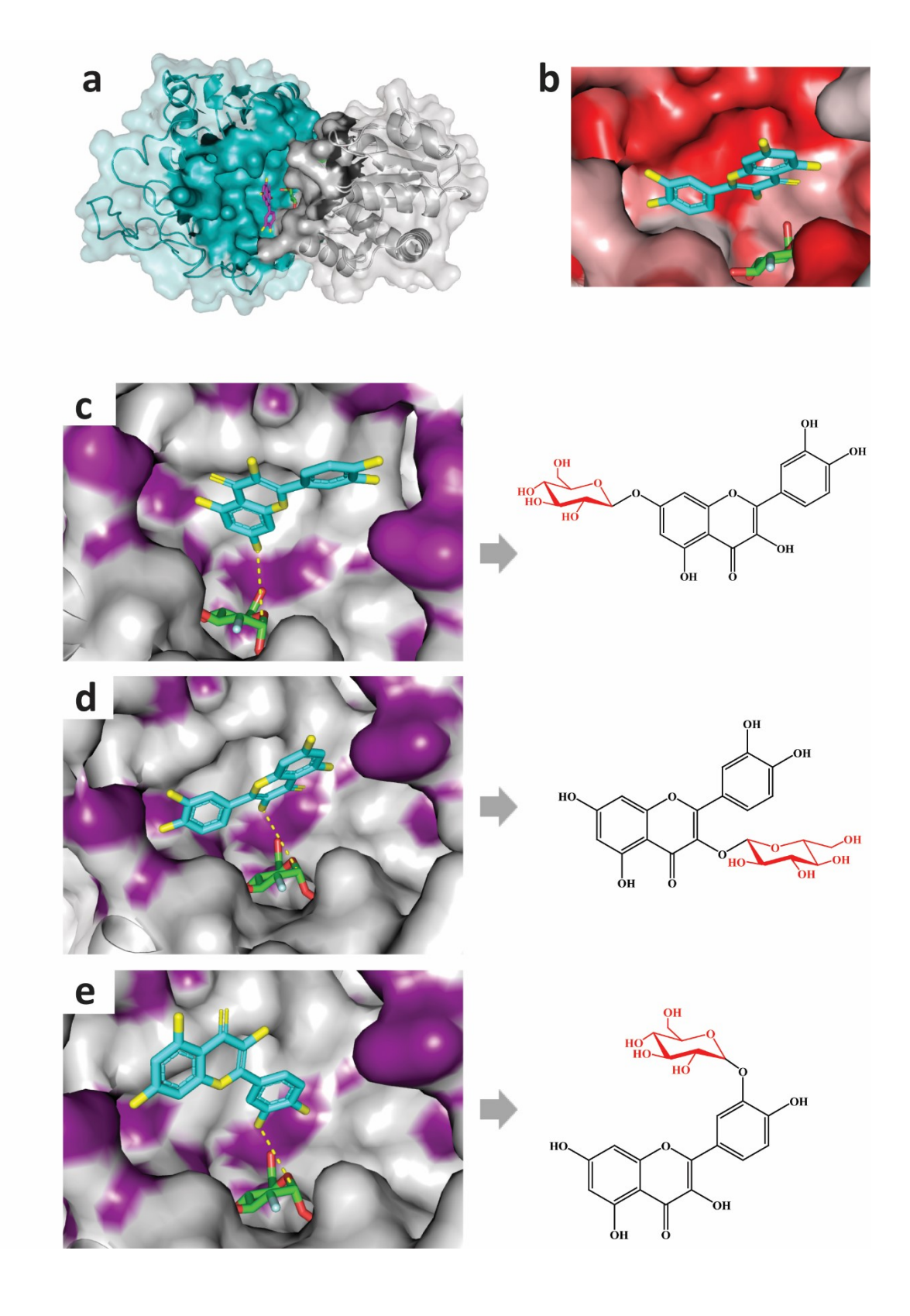
Fig. 3





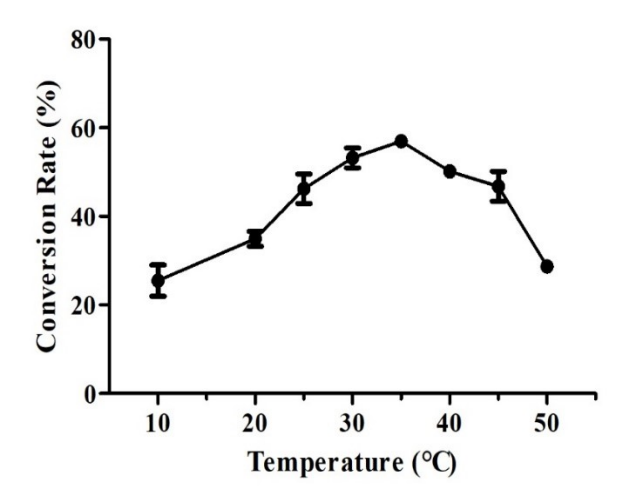


1001 Fig. 4

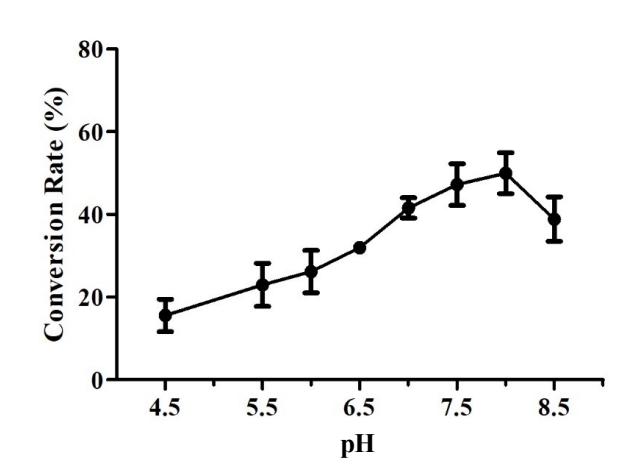


1007 Fig. 5

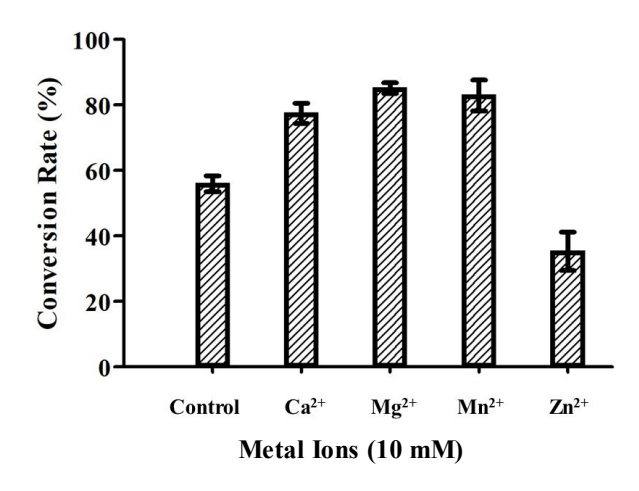
a



b



c



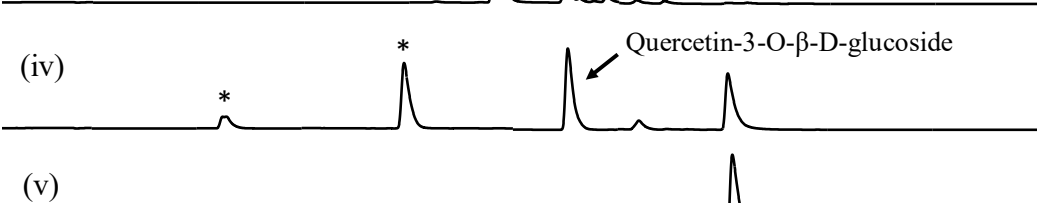
1009 Fig. 6

a



(ii) Quercetin-/-O-p-D-glucoside

(iii)



mAU

1400

1200

1000

800 -

600 -

400 -

200 -

b

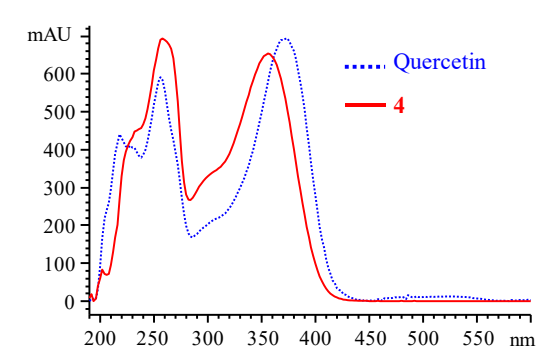
5 10 15 20

.... Quercetin

ю

3

c



30

min

25

Quercetin

1012 d

OH HO HO 7

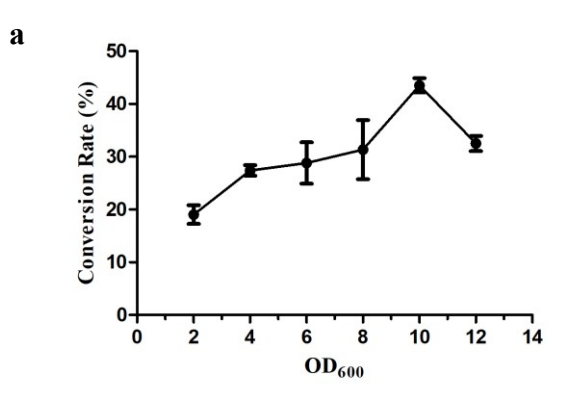
200 250 300 350 400 450 500 550 nm

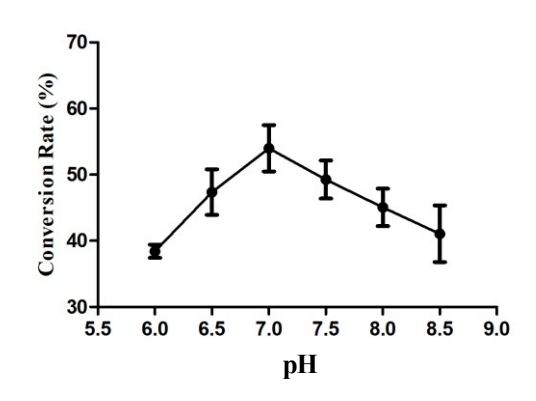
3

OH OHOOH OH

1013

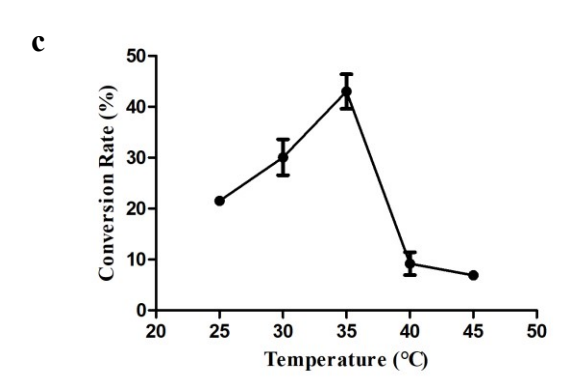
1014 Fig. 7

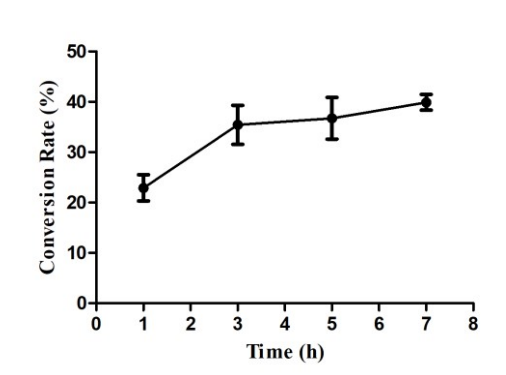


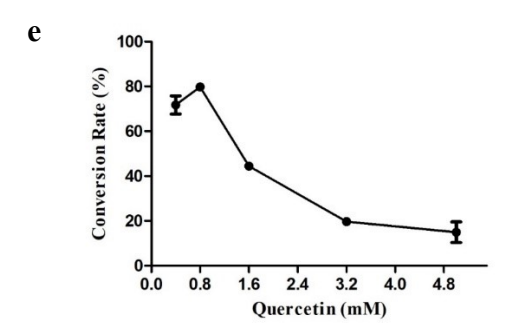


b

d



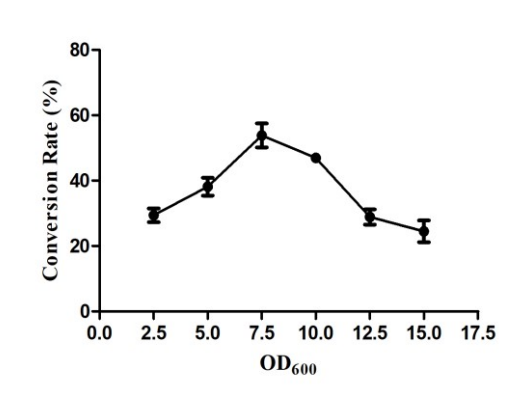


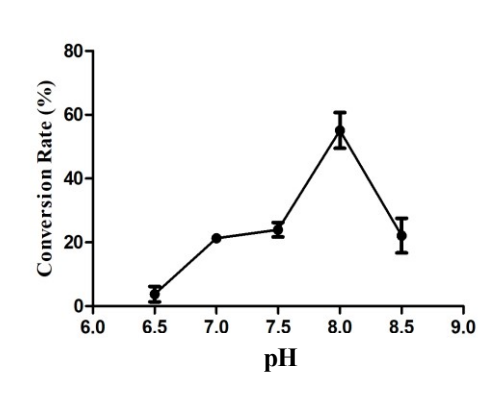


1018 Fig. 8

1024

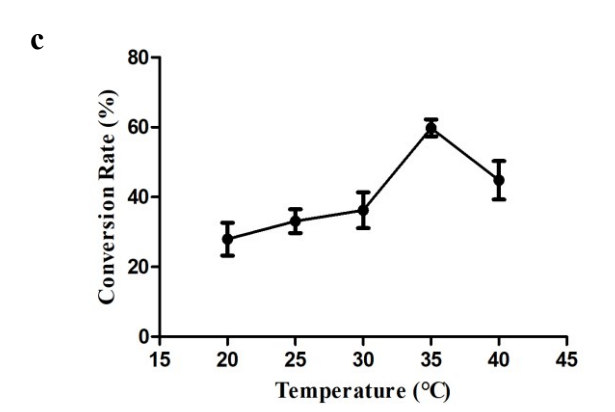
a

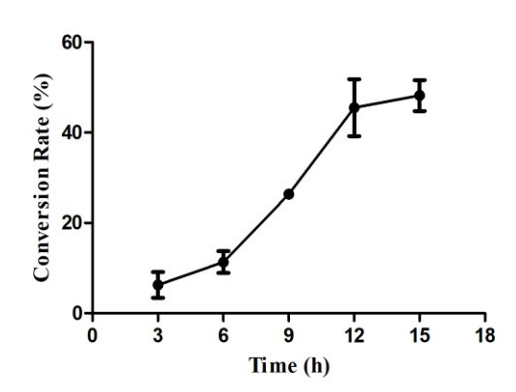


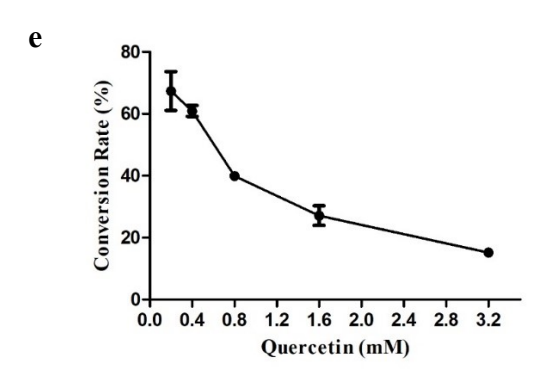


b

d







1025 Fig. 9

1026